J. Fluid Mech. (2009), *vol.* 639, *pp.* 479–507.
doi:10.1017/S0022112009991273

Mechanisms underlying transient growth of planar perturbations in unbounded compressible shear flow

NIKOLAOS A. BAKAS†

Department of Physics, National and Kapodistrian University of Athens, Building IV Panepistimiopolis, 15784 Athens, Greece

(Received 16 November 2008; revised 19 July 2009; accepted 19 July 2009; first published online 16 October 2009)

Non-modal mechanisms underlying transient growth of propagating acoustic waves and non-propagating vorticity perturbations in an unbounded compressible shear flow are investigated, making use of closed form solutions. Propagating acoustic waves amplify mainly due to two mechanisms: growth due to advection of streamwise velocity that is typically termed as the lift-up mechanism leading for large Mach numbers to an almost linear increase in streamwise velocity with time and growth due to the downgradient irrotational component of the Reynolds stress leading to linear growth of acoustic wave energy for large times. Synergy between these mechanisms along with the downgradient solenoidal component of the Reynolds stress produces large and robust energy amplification.

On the other hand, non-propagating vorticity perturbations amplify due to kinematic deformation of vorticity by the mean flow. For weakly compressible flows, an initial vorticity perturbation abruptly excites acoustic waves with exponentially small amplitude, and the energy gained by vorticity perturbations is transferred back to the mean flow. For moderate Mach numbers, a strong coupling between vorticity perturbations and acoustic waves is found with the energy gained by vorticity perturbations being transferred to acoustic waves that are abruptly excited by the vortex.

Calculation of the optimal perturbations for a viscous flow shows that for low Mach numbers, acoustic wave excitation by vorticity perturbations and the subsequent growth of acoustic waves leads to robust energy growth of the order of Reynolds number, while for large Mach numbers, synergy between the lift-up mechanism and the downgradient solenoidal component of the Reynolds stress dominates the growth and leads to a comparable large amplification of streamwise velocity.

1. Introduction

A comprehensive understanding of the stability of compressible shear flows is a fundamental problem in fluid mechanics and has been the subject of both theoretical and practical interest in astrophysics and engineering. Applications include transition to turbulence and the eventual flow breakdown of supersonic and hypersonic boundary layers arising in aerodynamic design problems (Mack 1965, 1975; Blumen, Drazin & Billings 1975), maintenance of turbulence in accretion disks around massive

† Email address for correspondence: nikos.bakas@gmail.com

bodies (Ioannou & Kakouris 2001) and stability of supersonic shear layers in astrophysical jets (Hardee 1979; Choudhury & Lovelace 1984).

Modal stability theory considering the exponential temporal growth of small perturbations in viscous boundary layers (Blumen *et al.* 1975; Mack 1975) and bounded shear flows (Duck, Erlebacher & Hussaini 1994; Hu & Zhong 1998) has been widely studied in the past. However, a large number of studies has shown that modal stability analysis provides an inadequate description of instability and turbulent transition, as it addresses only the large-time asymptotic fate of perturbations and has to be complemented by the analysis of transiently growing perturbations (Farrell 1984, 1988; Gustavsson 1991; Butler & Farrell 1992; Reddy & Henningson 1993; Buizza & Palmer 1995; Kim & Lim 2000). Such rapid perturbation energy amplification arises from the non-orthogonality of the modal spectrum and is possible even in the parameter space that is stable according to modal stability theory (Reddy, Schmid & Henningson 1993; Trefethen *et al.* 1993). As a result, a novel way of describing fluid stability for incompressible flows quickly emerged (see Farrell & Ioannou 1996, Schmid & Henningson 2001 and Schmid 2007 for a review). Application of these new concepts and techniques in compressible flows (Hanifi, Schmid & Henningson 1996; Farrell & Ioannou 2000; Malik, Alam & Dey 2006) found a large transient perturbation energy growth that dominates over modal growth except in the limit of long time and concluded that both modal and non-modal processes have to be taken into account in order to assess the stability of compressible shear flows at finite time.

Hanifi *et al.* (1996) addressed non-modal growth in compressible boundary layers and found that the maximum transient energy growth occurs for structures which are independent of the streamwise direction and that this growth increases with both the Reynolds and Mach numbers. Furthermore, Hanifi & Henningson (1998) showed that the mechanism underlying transient growth in the bounded flow is similar to the inviscid algebraic instability for streamwise disturbances found by Ellingsen & Palm (1975) in which the streamwise perturbation velocity grows linearly with time. Malik *et al.* (2006) studied non-modal transient energy growth for the compressible plane Couette flow of a perfect gas model for three-dimensional disturbances and found in contrast to the results for boundary layers that the optimal energy growth decreases with increasing Mach number for a given Reynolds number. They also found that optimal velocity patterns correspond to pure streamwise vortices only for large Mach numbers, with modulated streamwise vortices being the optimal patterns for low to moderate values of the Mach number, implying that there is an additional growth mechanism involved.

Further insight into the mechanisms underlying transient growth can be gained to a first approximation through study of a relatively simple unbounded constant-shear-flow model. Even though such an unbounded flow does not support modal solutions, it has the advantage of allowing analytic solutions that consist of a linear superposition as a Fourier integral of space periodic waves with time-dependent wavenumber and amplitude, typically known as Kelvin modes (Kelvin 1887) or shear waves. Lord Kelvin first introduced this solution for an unbounded, viscous shear flow (Kelvin 1887), and since then it has been generalized for incompressible flows incorporating density stratification (Phillips 1966; Hartman 1975; Criminale & Cordova 1986; Farrell & Ioannou 1993*b*) and Coriolis force (Yamagata 1976; Farrell 1982; Boyd 1983; Tung 1983; Vanneste & Yavneh 2004) and for compressible flows (Chagelishvili, Rogava & Segal 1994; Chagelishvili *et al.* 1997*a*,*b*; Farrell & Ioannou 2000). It has also been extended to non-parallel, time-dependent flows with spatially

uniform shearing rates by Craik & Criminale (1986) and to arbitrary flows by Lifschitz & Hameiri (1991) who developed a Wentzel–Kramers–Brillouin-like (WKB-like) stability method known as the geometrical optics stability method that examines the evolution of a highly localized perturbation in a Lagrangian reference frame moving with the unperturbed flow. Moreover, previous studies of incompressible flows (Farrell & Ioannou 1993*a*), of stably stratified flows (Farrell & Ioannou 1993*b*) and of compressible viscous flows (Farrell & Ioannou 2000) showed that this analytic solution for the unbounded flow captures most of the salient features of transient growth in the corresponding bounded flows as well.

Chagelishvili *et al.* (1994) studied an unbounded, compressible shear flow and found using the Kelvin mode formulation that for weak shear there are two classes of perturbations: aperiodic vorticity perturbations and propagating acoustic waves. Chagelishvili *et al.* (1997*a*) showed by numerical integration of the resulting equations for the time-dependent amplitude of the sheared disturbances that acoustic waves can extract mean flow energy as intensively as vortex perturbations do and that in contrast to vortex perturbations, the energy of acoustic waves grows linearly with time in the inviscid limit as they are sheared over by the mean flow. Chagelishvili *et al.* (1997*a*) also found that in weak shear flows acoustic wave temporal evolution is adiabatic, while in flows with moderate values of the Mach number the adiabatic characteristic of perturbation evolution is lost and the energy exchange process strongly depends on the phase of the waves as they enter the non-adiabatic region. Transient energy growth of acoustic waves for large Mach numbers was investigated by Farrell & Ioannou (2000) who distinguished two phases of growth: a large initial growth due to the solenoidal component of the Reynolds stress that is downgradient for early times and a subsequent growth due to downgradient Reynolds stresses associated with the irrotational component of the velocity fields. Farrell & Ioannou (2000) also found that the late-time growth that they identified as the adiabatic growth of Chagelishvili *et al.* (1997*a*) is not sustained in viscous flows due to increased viscous damping of the perturbations obtaining an ever-decreasing length scale. In this study, a thorough investigation of transient growth for all Mach numbers will be performed; the mechanisms underlying perturbation energy growth in both the adiabatic and the non-adiabatic regime will be identified; and their relevance in the evolution of both the inviscid and the viscous flow will be discussed.

Apart from the interaction of acoustic waves with the mean flow, Chagelishvili *et al.* (1997*b*) found an additional interaction leading to transient growth. Chagelishvili *et al.* (1997*b*) found that the aperiodic vorticity perturbations gain energy from the shear flow and subsequently transfer their energy to propagating acoustic waves that are abruptly excited by the vortex. This vortex wave–acoustic wave interaction is a dynamical process in compressible, turbulent fluids, playing an important role in acoustic destabilization of laminar flows (Broadbent & Moore 1979; Ho & Huerre 1984), in prediction of the form of sonic bangs produced by supersonic aircraft (Williams & Howe 1973) and in conversion of vortices to gravity spiral waves taking place in accretion disks (Tevzadze, Chagelishvili & Zahn 2008). It is therefore of interest to support the numerical evidence of this wave excitation process with analytic results providing asymptotic estimates for the amplitude of the generated acoustic waves. In this study we address this problem by using exponential–asymptotic techniques to estimate the amplitude of the generated acoustic waves appearing abruptly during the evolution of a vortex.

The goal of this study is to identify all the transient growth mechanisms occurring in an unbounded, compressible shear flow and study their synergy using closed form

solutions to the initial value problem. Using the Kelvin wave formulation (Kelvin 1887) and non-modal stability analysis tools (Farrell & Ioannou 1996; Schmid 2007), we investigate the mean flow–acoustic wave interactions and the vorticity wave–acoustic wave interactions and find the structures amplifying most in energy. The effect of boundaries and the relevance of these growth mechanisms in compressible shear flow instability will be investigated in a follow-up study.

This paper is organized as follows. In § 2 we describe the linear evolution equations for planar perturbations in a compressible shear flow and briefly discuss the possible energy transfers between the perturbations and the mean flow. In § 3, we elaborate on the mechanisms for energy growth of the acoustic waves, as well as their synergy. Interactions between non-propagating vorticity perturbations and acoustic waves are studied in § 4, while the optimally growing perturbations are identified in § 5. We finally end with a brief discussion in § 6 and our conclusions in § 7.

2. Growth mechanisms of sheared waves

2.1. *Evolution equations for planar perturbations*

Consider a flow with mean velocity $U(y)=y$ of constant shear in a polytropic fluid (i.e. pressure related to the spatially uniform density ρ by $P=K\rho^{\gamma}$). Perturbations of streamwise velocity u and cross-stream velocity v are superposed on the background flow, and perturbations of pressure p are superposed on the mean pressure field. The linearized, non-dimensional momentum and pressure equations governing the evolution of small perturbations are

$$(\partial_t + U(y)\partial_x)u + v = -\partial_x p, \tag{2.1}$$

$$(\partial_t + U(y)\partial_x)v = -\partial_y p, \tag{2.2}$$

$$(\partial_t + U(y)\partial_x)p = -\frac{1}{M^2}(\partial_x u + \partial_y v). \tag{2.3}$$

Spatial scales and velocities are non-dimensionalized by typical values of length L and mean flow velocity V_0 respectively. Time is non-dimensionalized by the shear L/V_0, and pressure is non-dimensionalized by ρV_0^2. The Mach number, measuring the ratio of the characteristic flow speed to the speed of sound, c_s, is $M=V_0/c_s$.

Following a generalization of the Kelvin modes (Kelvin 1887), we seek solutions of the form $[u, v, p]=[\hat{u}(t), \hat{v}(t), \hat{p}(t)]\mathrm{e}^{\mathrm{i}kx+\mathrm{i}(m-kt)y}$ with time-varying cross-stream wavenumber $m-kt$ that is equivalent to transforming (2.1)–(2.3) into the convected coordinate frame of reference (Phillips 1966) that is moving with the background flow ($\xi=x-yt$). This solution form offers the advantage of allowing analytic solutions, as it reduces the original partial differential equations to the following set governing the evolution of the time-dependent Fourier amplitudes $[\hat{u}(t), \hat{v}(t), \hat{p}(t)]$:

$$\frac{\mathrm{d}\hat{u}}{\mathrm{d}t} = -\mathrm{i}k\hat{p} - \hat{v}, \tag{2.4}$$

$$\frac{\mathrm{d}\hat{v}}{\mathrm{d}t} = -\mathrm{i}(m-kt)\hat{p}, \tag{2.5}$$

$$\frac{\mathrm{d}\hat{p}}{\mathrm{d}t} = -\frac{\mathrm{i}k}{M^2}\hat{u} - \frac{\mathrm{i}(m-kt)}{M^2}\hat{v}. \tag{2.6}$$

It can be readily shown from (2.4)–(2.6) that the Fourier component of the quantity $q=\partial_x v-\partial_y u+M^2 p$ is conserved:

$$\hat{q}(t) = \mathrm{i}k\hat{v}(t) - \mathrm{i}(m-kt)\hat{u}(t) + M^2\hat{p}(t) = \hat{q}(0). \tag{2.7}$$

This conserved quantity is similar to potential vorticity in stratified flows, as $M^2 p$ is the term associated with velocity divergence and with stretching and shrinking of vorticity columns through compressible expansion or contraction. Using (2.7) and combining (2.4)–(2.6) reduces (2.4)–(2.6) to a single second-order differential equation for $\hat{p}$:

$$\frac{\mathrm{d}^2\hat{p}}{\mathrm{d}t^2} + \frac{2k(m-kt)}{K^2}\frac{\mathrm{d}\hat{p}}{\mathrm{d}t} + \left(\frac{K^2}{M^2} + \frac{2k^2}{K^2}\right)\hat{p} = \frac{2\hat{q}(0)k^2}{M^2K^2}, \tag{2.8}$$

where $K(t)^2 = k^2 + (m-kt)^2$ is the square of the time-dependent total wavenumber of the plane wave. As will be shown in the sequel, the solution of the homogeneous restriction of (2.8) describes the dynamics of transient acoustic waves, whereas the particular solution involves the interaction between propagating acoustic waves and non-propagating vortical perturbations. We will therefore study the solution to the homogeneous restriction of (2.8) (§ 3) and the particular solution (§ 4) separately.

2.2. *Energy transfers between the perturbations and the mean flow*

Insight into perturbation energetics can be gained by considering the transfers of energy between the perturbations and the mean flow. Unfortunately, unlike the case of incompressible flows, there is no obvious choice for a natural energy norm measuring perturbation size for compressible flows. A possible choice would be Myers's acoustic energy corollary (Myers 1991) that is valid to second order:

$$E_M = (1/2)(\overline{u^2+v^2}) + (M^2/2)\overline{p^2} + M^2\overline{pu}U,$$

where the overbar denotes an average in the streamwise direction. However the energy corollary for plane wave sheared disturbances in the convected coordinates is restricted to be homogeneous in y, and E_M depending explicitly on $U(y)$ cannot be used. Instead we follow Mack (1969) and all previous studies addressing short-time growth in compressible flows (Chagelishvili *et al.* 1994; Hanifi *et al.* 1996; Chagelishvili *et al.* 1997*a*,*b*; Hanifi & Henningson 1998; Farrell & Ioannou 2000; Malik *et al.* 2006) in choosing an energy norm satisfying the requirement that the spatial average of the rate of pressure-related work, i.e. the compression work, does not contribute to the energy density evolution, since compression work is conservative. It can be readily shown from (2.2)–(2.3) that the proper choice eliminating pressure work is $E = (1/2)(\overline{u^2+v^2}) + (M^2/2)\overline{p^2}$, where the overbar denotes an average over space, and that the energy density grows/decays because of the energy source associated with the Reynolds stress:

$$\frac{\mathrm{d}E}{\mathrm{d}t} = -\overline{uv},$$

where the overbar denotes again an average over space. In order to gain further insight into the energy growth mechanisms, we follow Farrell & Ioannou (2000) and decompose the velocity perturbations into an irrotational and a solenoidal part: $(u, v) = \nabla\phi + \nabla \times (\psi\hat{\boldsymbol{k}})$, where $\hat{\boldsymbol{k}}$ is the unit vector perpendicular to the flow, ϕ is the velocity potential of the irrotational component and ψ is the streamfunction of the solenoidal component. In the convected coordinate frame of reference, this equation reduces to

$$[\hat{u}(t), \hat{v}(t)] = [\mathrm{i}k\hat{\phi}(t) + \mathrm{i}(m-kt)\hat{\psi}(t), \mathrm{i}(m-kt)\hat{\phi}(t) - \mathrm{i}k\hat{\psi}(t)], \tag{2.9}$$

where $\hat{\phi}$, $\hat{\psi}$ are the time-dependent Fourier amplitudes, such that $[\phi, \psi] = [\hat{\phi}(t), \hat{\psi}(t)]\mathrm{e}^{\mathrm{i}kx+\mathrm{i}(m-kt)y}$. Decomposing the Reynolds stress into solenoidal and irrotational

parts as well yields

$$\frac{\mathrm{d}E}{\mathrm{d}t} = \underbrace{\frac{1}{2}k(m-kt)|\hat{\psi}|^2}_{\overline{uv}_{Orr}} \underbrace{-\frac{1}{2}k(m-kt)|\hat{\phi}|^2}_{\overline{uv}_{comp}} \underbrace{-\frac{(m-kt)^2}{2}Re(\hat{\phi}^*\hat{\psi})}_{\overline{uv}_{lift}} + \underbrace{\frac{k^2}{2}Re(\hat{\phi}\hat{\psi}^*)}_{\overline{uv}_{interf}}, \quad (2.10)$$

where

$$E = \frac{1}{4}(|\hat{u}|^2 + |\hat{v}|^2 + M^2|\hat{p}|^2) \quad (2.11)$$

is the energy density of a sheared plane wave.

The solenoidal term $\overline{uv}_{Orr}$ is the sole energy source for incompressible flow. In that case, that is for incompressible flow, the cross-stream component of vorticity is conserved (Kelvin 1887; Orr 1907) and the time-dependent Fourier amplitudes are given by

$$[\hat{u}_{M0}(t), \hat{v}_{M0}(t), \hat{p}_{M0}(t)] = \left[-(m/k-t)\hat{v}_{M0}(t), \frac{-\mathrm{i}k\hat{q}(0)}{k^2+(m-kt)^2}, \frac{2k^2\hat{q}(0)}{(k^2+(m-kt)^2)^2}\right], \quad (2.12)$$

where $\hat{q}(0) = \mathrm{i}k\hat{v}(0) - \mathrm{i}m\hat{u}(0)$ is the initial cross-stream vorticity. As the phase lines of a vorticity wave are kinematically deformed by the shear flow, the cross-stream and streamwise velocity fields have to grow if the phase lines are tilted against the shear ($m - kt > 0$) in order to conserve vorticity. The result is a very large cross-stream velocity perturbation peaking at $t = m/k$. The solenoidal term $\overline{uv}_{Orr}$ is positive, and perturbation energy grows. For later times, the phase lines tilt with the shear ($m - kt < 0$); the solenoidal term becomes an energy sink; and perturbation energy decays. This is the mechanism of growth in two-dimensional shear discussed by Orr (1907), and we will refer to it as the Orr mechanism.

The second term arising from the irrotational component of the velocity field exists only for compressible flow and has the opposite effect on perturbation energy. That is for plane wave perturbations with phase lines tilted against the shear ($m - kt > 0$), the irrotational term $\overline{uv}_{comp}$ is an energy sink, while for later times it becomes an energy source and is expected to play a significant role for large times. The last two terms ($\overline{uv}_{lift}$, $\overline{uv}_{interf}$) arise from the interaction of the solenoidal components with the irrotational components of the velocity fields. The third term $\overline{uv}_{lift}$ is the sole energy source/sink for streamwise-independent perturbations, while numerical integration of the equations have shown that in all the cases considered the last term is small and does not contribute significantly to the energy evolution.

We elaborate further on $\overline{uv}_{lift}$ and $\overline{uv}_{comp}$ in the next section, where we first study two separate limits permitting closed form solutions and illuminating the growth mechanisms arising for streamwise-independent perturbations and for nearly irrotational perturbations respectively. Using the intuition gained, we then treat the evolution of acoustic waves in the general case.

3. Homogeneous solution and energy growth of acoustic waves

3.1. *Growth of perturbations with no streamwise variation*

Consider first the limit of streamwise uniform solutions ($k = 0$) for which $\hat{q}(0) = 0$. Since there is no pressure gradient force in the streamwise direction, the total streamwise velocity (perturbation and mean) is conserved. Such perturbations can therefore grow by advection of mean streamwise velocity by perturbation cross-stream

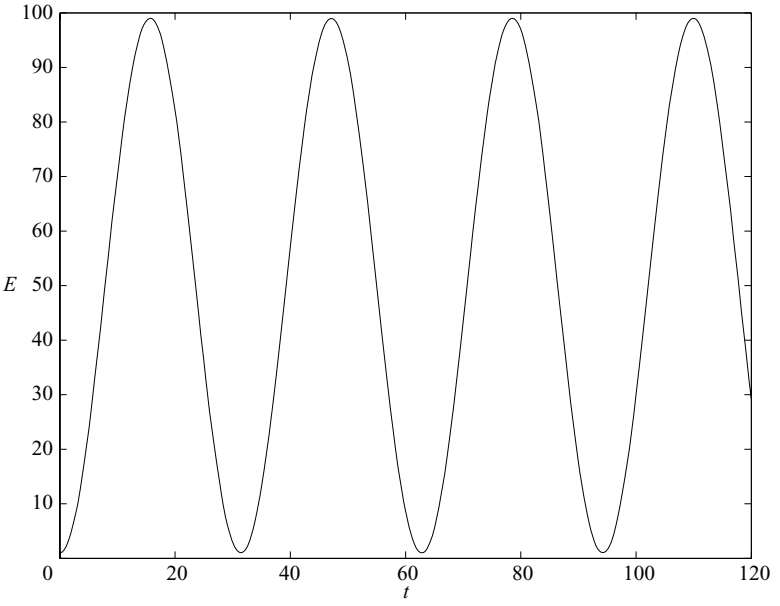

FIGURE 1. Energy evolution of a streamwise-independent plane wave with $m = 5$ and $[\hat{u}(0), \hat{v}(0), \hat{p}(0)] = [0, 2, 0]$. The Mach number is $M = 50$.

velocity to regions of lower/higher background velocity. For an incompressible flow, the cross-stream perturbation velocity is constant, and this so-called lift-up mechanism leads to linear growth of streamwise velocity (Ellingsen & Palm 1975; Landhal 1980; Farrell & Ioannou 1993*a*; Reddy & Henningson 1993) and produces pronounced perturbation streamwise streaks. For a compressible boundary layer flow and in the absence of a pressure gradient force, the lift-up mechanism results in linear growth of density and temperature in addition to linear growth of streamwise velocity (Hanifi & Henningson 1998).

For the compressible polytropic fluid considered in this study, cross-stream motion is opposed by the pressure gradient force, and the solution of (2.4)–(2.6) for $k = 0$, $m \neq 0$ and initial conditions satisfying $\hat{q}(0) = 0$ is

$$\hat{u}(t) = -\frac{\mathrm{i}}{2}\left(\frac{m\hat{p}(0)}{\omega_0^2} - \frac{\hat{v}(0)}{\omega_0}\right)\mathrm{e}^{\mathrm{i}\omega_0 t} - \frac{\mathrm{i}}{2}\left(\frac{m\hat{p}(0)}{\omega_0^2} + \frac{\hat{v}(0)}{\omega_0}\right)\mathrm{e}^{-\mathrm{i}\omega_0 t}, \tag{3.1}$$

$$\hat{v}(t) = \frac{1}{2}\left(\hat{v}(0) - M\hat{p}(0)\right)\mathrm{e}^{\mathrm{i}\omega_0 t} + \frac{1}{2}\left(\hat{v}(0) + M\hat{p}(0)\right)\mathrm{e}^{-\mathrm{i}\omega_0 t}, \tag{3.2}$$

$$\hat{p}(t) = \frac{1}{2}\left(\hat{p}(0) - \frac{\hat{v}(0)}{M}\right)\mathrm{e}^{\mathrm{i}\omega_0 t} + \frac{1}{2}\left(\hat{p}(0) + \frac{\hat{v}(0)}{M}\right)\mathrm{e}^{-\mathrm{i}\omega_0 t}, \tag{3.3}$$

where

$$\omega_0 = m/M. \tag{3.4}$$

All fields vary harmonically in time with the frequency ω_0, satisfying the dispersion relation of an acoustic wave that propagates freely in a quiescent flow. The two terms in (3.1)–(3.3) therefore represent two counter-propagating acoustic waves in the y-plane. The energy evolution of an initial disturbance that is given by (2.11) is shown in figure 1. The observed oscillation is the result of interference of the infinitely extending plane wave solutions considered in this study. Further investigation of (2.11) reveals

that $(|\hat{v}|^2 + M^2|\hat{p}|^2)$ is constant. Therefore, the observed energy growth can be traced to streamwise velocity growth due to the lift-up mechanism discussed in the beginning of this section. As a result, streamwise-independent perturbations propagating within a shear region can produce large streamwise streaks that are regions susceptible to shear instability. In contrast to the previous studies of the lift-up mechanism for incompressible (Ellingsen & Palm 1975; Landhal 1980; Farrell & Ioannou 1993*a*; Reddy & Henningson 1993) and compresible boundary layers (Hanifi & Henningson 1998), streamwise velocity growth is not linear, as cross-stream motion is opposed by the pressure gradient force limiting cross-stream advection. It is therefore of interest to identify the perturbations leading to the largest energy growth that can be achieved, as the maximum growth provides a measure of the strength of the lift-up mechanism and the optimal perturbations identify the initial structures that are expected to dominate perturbation dynamics in the linear limit. In Appendix A we obtain closed form solutions for the optimal streamwise-independent perturbations maximizing energy growth at a specified time T_{opt}. That is for a plane wave perturbation of given wavenumber m, we calculate the initial conditions leading to maximum energy $E^m_{opt}(T_{opt})$ at the specified time T_{opt} under the constraint of unit initial energy. The optimal perturbations are then obtained by calculating the wavenumber m maximizing E^m_{opt}. We find that the energy growth is maximized for non-propagating spatially uniform perturbations ($m=0$), as in this limit there is no pressure gradient force leading to unopposed constant advection in the cross-stream direction and to linear growth of streamwise velocity with time. However, the optimal growth remains large for propagating disturbances having $m/M \ll 1$ (resulting in a weak pressure gradient force) and asymptotes to $1 + T^2_{opt}$ for large optimization times. The optimal initial perturbations producing this growth are cross-stream velocity perturbations. Therefore, the lift-up mechanism is optimally initiated by a cross-stream velocity perturbation and is proportional to M/m that is a measure of the extent of the maximum cross-stream displacement. The lift-up mechanism is consequently more efficient for supersonic flows.

3.2. *Growth of acoustic waves in the limit of small Mach number*

We now investigate the energy growth of acoustic waves in the limit $M/k \ll 1$, that is when the period of the acoustic waves is much smaller than the advective time scale. Unless we are interested in waves with very short horizontal scales, this limit corresponds to weak shear flows or small Mach numbers, and we will hereafter refer to it as the small-Mach-number limit. Acoustic wave evolution for weak shear flows or nearly incompressible flows has also been studied by Chagelishvili *et al.* (1994, 1997*a*) who found analytic asymptotic solutions in this case. A slightly different derivation of the asymptotic solutions admitted in this limit follows. Consider (2.8) for $\hat{q}(0)=0$:

$$\frac{\mathrm{d}^2\hat{p}}{\mathrm{d}t^2} + \frac{2k(m-kt)}{K^2}\frac{\mathrm{d}\hat{p}}{\mathrm{d}t} + \left(\frac{K^2}{M^2} + \frac{2k^2}{K^2}\right)\hat{p} = 0. \tag{3.5}$$

For $M/k \ll 1$, (3.5) admits the asymptotic WKB solution

$$\hat{p}(t) = \sqrt{K(t)}\left(A_+ \mathrm{e}^{(\mathrm{i}/M)\int_0^t K(s)\,\mathrm{d}s} + A_- \mathrm{e}^{(-\mathrm{i}/M)\int_0^t K(s)\,\mathrm{d}s}\right), \tag{3.6}$$

where

$$A_\pm = \frac{1}{2\sqrt{K(0)}}\left(\hat{p}(0) \mp \frac{k\hat{u}(0) + m\hat{v}(0)}{MK(0)}\right).$$

Since the solution considered is of the form $p = \hat{p}(t)\mathrm{e}^{\mathrm{i}kx+\mathrm{i}(m-kt)y}$, the two terms in (3.6) represent two counter-propagating acoustic waves with streamwise wavenumber k and time-dependent cross-stream wavenumber $m - kt$. The velocity Fourier amplitudes for each of these waves are obtained as follows: (2.7) yields for $\hat{q}(0) = 0$ and in the limit $M/k \ll 1$

$$\hat{v}(t) = \frac{m - kt}{k}\hat{u}(t) + O(M^2). \tag{3.7}$$

Substituting (3.6) and (3.7) into (2.6) yields the following in the limit $M/k \ll 1$:

$$[\hat{u}(t), \hat{v}(t)] = -[k, m - kt]\frac{MA_{\pm}}{\sqrt{K(t)}}\mathrm{e}^{\pm(\mathrm{i}/M)\int_0^t K(s)\,\mathrm{d}s} + O(M^2). \tag{3.8}$$

Perturbations are irrotational to first order in this limit, as by substituting (3.8) into (2.9) and solving for $\hat{\phi}$, $\hat{\psi}$ we obtain

$$\hat{\phi}(t) = \frac{\mathrm{i}MA_{\pm}}{\sqrt{K}}\mathrm{e}^{\pm(\mathrm{i}/M)\int_0^t K(s)\,\mathrm{d}s} + O(M^2), \tag{3.9}$$

while $\hat{\psi}(t) \sim O(M^2)$. The energy density for each of these waves is then given by substituting (3.6) and (3.8) into (2.11):

$$E(t) = \frac{M^2}{2}\left|A_{\pm}\sqrt{K}\mathrm{e}^{\pm(\mathrm{i}/M)\int_0^t K(s)\,\mathrm{d}s}\right|^2 = \frac{M^2}{2}K(t)|A_{\pm}|^2.$$

Therefore, the ratio of the energy of these acoustic waves to their time-dependent frequency $K(t)$ is an adiabatic invariant (Chagelishvili *et al.* 1997*a*), and the overall energy growth for each of these waves,

$$\frac{E(t)}{E(0)} = \frac{K(t)}{K(0)} = \sqrt{\frac{k^2 + (m - kt)^2}{k^2 + m^2}}, \tag{3.10}$$

is shown in figure 2. The energy sources and sinks are given by substituting (3.9) into (2.10) to obtain

$$\frac{\mathrm{d}E}{\mathrm{d}t} = -\frac{1}{2}k(m - kt)|\hat{\phi}|^2 + O(M|\hat{\phi}|) = -\frac{k(m - kt)M^2}{2\sqrt{k^2 + (m - kt)^2}}.$$

That is the acoustic wave energy grows/decays to first order because of the irrotational part of the Reynolds stress. For an initial perturbation with $m/k > 0$, the irrotational part of the Reynolds stress is upgradient for $t < m/k$ and the energy initially decays, whereas for $t > m/k$ its phase lines tilt with the shear and the Reynolds stress is downgradient leading to energy growth. For an initial perturbation with $m/k < 0$, the irrotational part of the Reynolds stress is downgradient leading to monotonic energy growth. This is the adiabatic growth mechanism discussed in Chagelishvili *et al.* (1997*a*) for three-dimensional perturbations and in Farrell & Ioannou (2000) for planar perturbations. The salient characteristic of this mechanism is that the acoustic waves extract energy from the mean flow when their constant-phase lines are tilted towards the shear, unlike advection waves in incompressible shear flows that are able to extract energy due to the solenoidal part of the Reynolds stress, uv_{Orr}, only when their phase lines are tilted against the mean shear (Orr 1907). Moreover, for large times, the Reynolds stress saturates to a constant value and the energy grows linearly as $E \simeq t/\sqrt{1 + (m/k)^2}$. Therefore, the energy growth for large times is maximized for plane waves with phase lines tilted initially almost vertically ($m/k \ll 1$) in contrast to the case of incompressible shear flows in which the energy is maximized

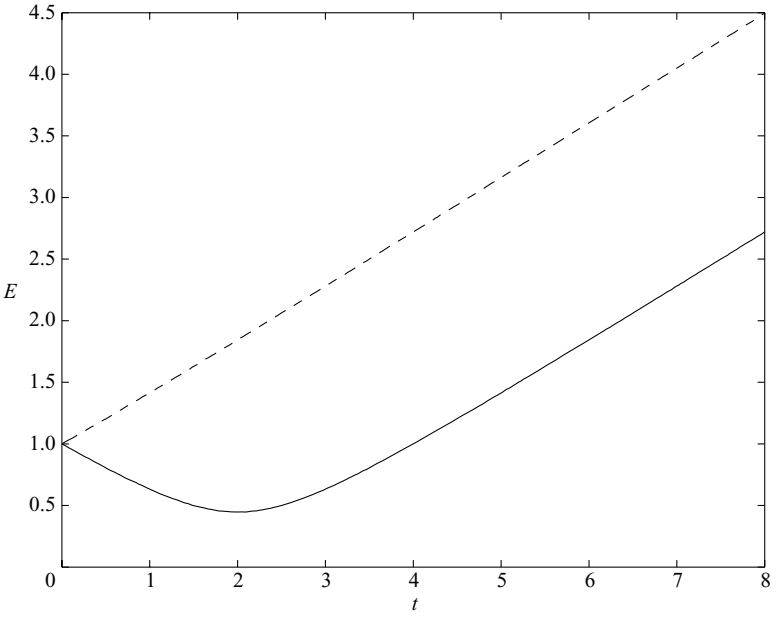

FIGURE 2. Energy evolution (given by (3.10)) for a plane wave with $(k, m) = (1, 2)$ (solid line) and $(k, m) = (1, -2)$ (dashed line). The Mach number is $M = 0.1$.

for shear waves with phase lines tilted almost horizontally ($m/k \gg 1$) to maximize the time available for growth (Farrell & Ioannou 1993*a*). It is also worth noting that the constant-phase lines of the optimal perturbations have an almost vertical orientation even as $M \to 0$. This result seems to be counterintuitive at first sight, since for suitable initial conditions the solution of the compressible equations converges to the solution of the incompressible equations as $M \to 0$ (Kreiss, Lorenz & Naughton 1991). However, it is an artefact of the condition $\hat{q}(0) = 0$ that was chosen, as in this case the incompressible solution is zero (see (2.12)), separating the growth arising from compressibility from the growth arising in incompressible flows. The case of $\hat{q}(0) \neq 0$ in which vorticity perturbations (advection waves) and acoustic waves coexist and interact is studied separately in §§ 4 and 5.

3.3. *Synergy between the growth mechanisms*

For stronger shear flows, or moderate Mach numbers, Chagelishvili *et al.* (1997*a*) found that energy growth of three-dimensional acoustic waves can be larger compared to the adiabatic growth studied in the previous subsection. Although through a qualitative analysis of energy exchange between fluid particles and the mean flow, Chagelishvili *et al.* (1997*a*) were able to heuristically explain such behaviour and invoked the lift-up mechanism as playing a role in this energy exchange, they did not provide robust evidence for the physical mechanisms underlying the excess growth. In this section, we show that energy growth in this regime occurs due to the synergy between the lift-up mechanism and the downgradient irrotational and solenoidal parts of the Reynolds stress. Consider first the case of a wave with phase lines tilted with the shear ($m/k < 0$). The solution is obtained by numerical integration of (3.5), and the energy evolution of the plane wave that is given by (2.11) is shown in figure 3 for a planar perturbation with initial wavenumbers $(k, m) = (0.2, -0.8)$ and $(k, m) = (0.2, -4)$. For $m = -4$, the extent of the cross-stream displacement that is

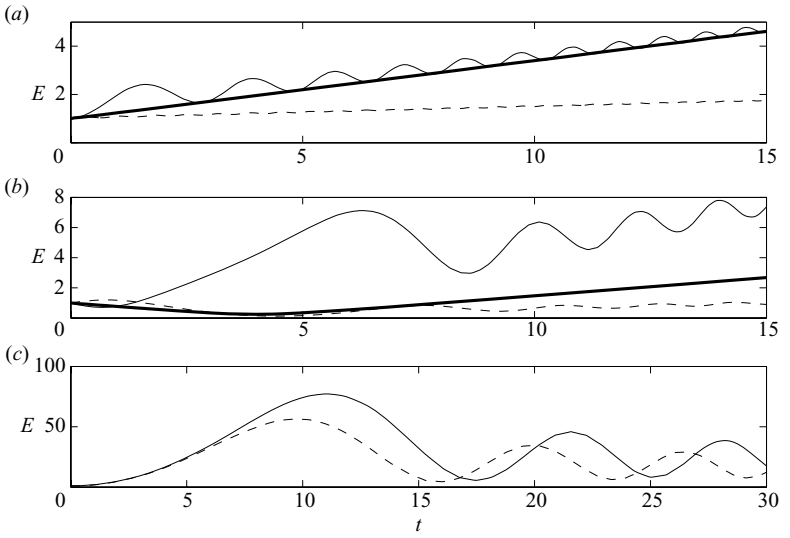

FIGURE 3. (*a*) Energy evolution of a plane wave with $(k, m) = (0.2, -0.8)$ (solid line) and $(k, m) = (0.2, -4)$ (dashed line) as given by (2.11). The initial conditions are $(\hat{u}(0), \hat{v}(0)) = (-0.1, 1)$, and the Mach number is $M = 1$. The energy evolution given by (3.10) for $m = -0.8$ is also shown (thick line) for reference. The corresponding curve for $m = -4$ coincides with the dashed line and is not shown. (*b*) Energy evolution of a plane wave with $(k, m) = (0.2, 0.8)$ given by (2.11) for initial conditions $(\hat{u}(0), \hat{v}(0)) = (-1, 0.5)$ (solid line) and $(\hat{u}(0), \hat{v}(0)) = (-1, -1.5)$ (dashed line). The Mach number is $M = 1$, and the energy evolution given by (3.10) for $m = 0.8$ is also shown (thick line). (*c*) Energy evolution of a plane wave with $(k, m) = (0.2, 0.2)$ (solid line) and $(k, m) = (0.2, -0.2)$ (dashed line) for initial conditions $(\hat{u}(0), \hat{v}(0)) = (0.2, 2)$ and Mach number $M = 10$. In all cases the initial pressure perturbation is given by (2.7) so that $\hat{q}(0) = 0$, and the perturbation amplitude is normalized to yield unit initial energy.

measured by $M/(m - kt)$ is small and growth of streamwise velocity due to the lift-up mechanism, which is proportional to $M/(m - kt)$ is weak. As a result, the energy evolution follows closely that predicted by (3.10) for $M/k \ll 1$. For the case with $m = -0.8$ the oscillations that appear to be superposed on the energy increase due to the irrotational Reynolds stress are solely due to streamwise velocity increase, indicating the presence of the lift-up mechanism. This result is illustrated in figure 4, where the evolution of each component of the Reynolds stress ($\overline{uv}_{Orr}$, $\overline{uv}_{com}$, $\overline{uv}_{lift}$) is shown. We can see that while the solenoidal component $\overline{uv}_{Orr}$ is very small and does not play a significant role in the energy evolution, $\overline{uv}_{lift}$ is of order one and along with the irrotational part that is downgradient for all times leads to the observed energy growth.

Consider now the case of waves with phase lines tilted against the shear ($m/k > 0$). A typical energy evolution of a planar wave with initial wavenumbers $(k, m) = (0.2, 0.8)$ is shown in figure 3(*b*). For initial conditions $(\hat{v}(0), \hat{v}(0)) = (-1, 0.5)$, the initial energy source of the downgradient solenoidal part of the Reynolds stress $\overline{uv}_{Orr}$ is unable to compensate for the energy loss arising from the upgradient irrotational component of the Reynolds stress $\overline{uv}_{comp}$ and the lift-up mechanism as shown in figure 4, and the energy decays rapidly for $t \sim m/k$. For later times $t > m/k$, the lift-up mechanism results in an equal growth and decay for each oscillation cycle, and the energy evolution is mainly determined by the downgradient irrotational component of the Reynolds stress alone (see figure 4). However, in this case, gradual amplification after $t > m/k$ is unable to compensate for the rapid loss at times $t \sim m/k$, and energy

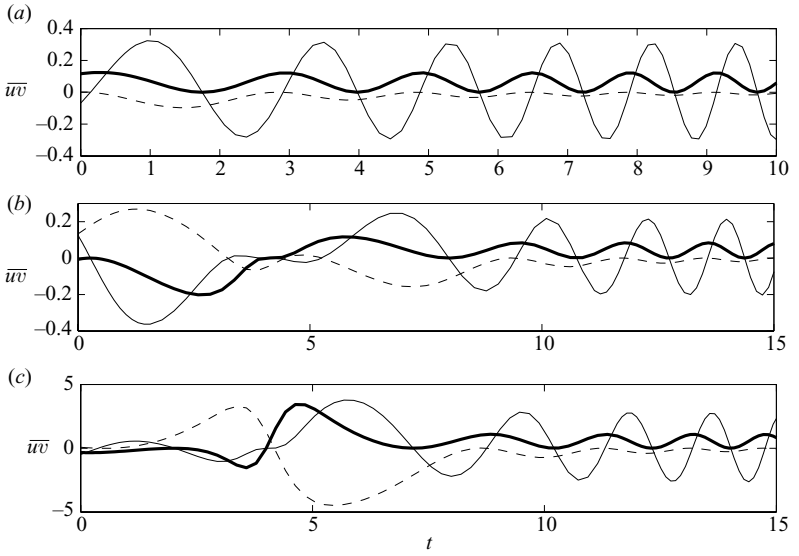

FIGURE 4. (*a*) Evolution of the irrotational component $\overline{uv}_{comp}$ (thick solid line), the advection component $\overline{uv}_{lift}$ (solid line) and the solenoidal component $\overline{uv}_{Orr}$ (dashed line) of the Reynolds stress for a plane wave with $(k, m) = (0.2, -0.8)$ and initial conditions $(\hat{u}(0), \hat{v}(0)) = (-0.1, 1)$. (*b*) The same as (*a*) for a plane wave with $(k, m) = (0.2, 0.8)$ and initial conditions $(\hat{u}(0), \hat{v}(0)) = (-1, 0.5)$. (*c*) The same as (*b*) for initial conditions $(\hat{u}(0), \hat{v}(0)) = (-1, -1.5)$. In all cases the Mach number is $M = 1$; the initial pressure perturbation is given by (2.7) so that $\hat{q}(0) = 0$; and the perturbation amplitude is normalized to yield unit initial energy.

density is overall decreased compared to the energy growth arising only from the irrotational component of the Reynolds stress.

For $(\hat{u}(0), \hat{v}(0)) = (-1, -1.5)$, the initial contribution of the solenoidal component of the Reynolds stress results in a large increase in cross-stream velocity as discussed in § 2.2. The increase in v leads not only to an initial energy growth but also to a large advection of u in the cross-stream direction initiating the lift-up mechanism that in turn causes a large increase of streamwise velocity right after $t \sim m/k$. This significant contribution of the lift-up mechanism in energy growth, along with the irrotational component of the Reynolds stress that is downgradient after $t = m/k$ (see figure 4), not only counteracts the energy sink associated with the solenoidal component after $t = m/k$ but also leads to a rapid energy density growth during this time interval and to an overall energy amplification that is significantly larger compared to the energy density growth arising only from the downgradient irrotational component of the Reynolds stress (see figure 3). Therefore, the synergy between the three growth mechanisms underlies the overall energy growth in what was termed in Chagelishvili *et al.* (1997*a*) the non-adiabatic regime.

The benefit from the synergism between the three growth mechanisms is also evident for large Mach numbers, for which the lift-up mechanism is very strong as discussed in § 3.1, and its contribution to energy growth is much larger compared to the other mechanisms (not shown). As illustrated in figure 3(*c*), energy growth of waves with $m/k > 0$ is larger than the corresponding energy growth of waves with opposite horizontal tilt ($m/k < 0$), for large Mach numbers as well. In this case, only part of the amplified streamwise velocity is converted into pressure perturbations. This results in very large streamwise velocity perturbations during the initial stage

of evolution that decay with time as $M/(m - kt)$ decreases monotonically. These perturbations could therefore lead to the formation of dynamically unstable regions if they persist long enough.

4. Particular solution and acoustic wave–vorticity wave interactions

In this section we focus on the particular solution that captures the interaction between propagating acoustic waves and non-propagating vorticity perturbations and is given by

$$p_{part} = \frac{2k^2\hat{q}(0)}{M^2} p_- \int_0^t \frac{p_+(s)}{K^2(s)W(s)}\,\mathrm{d}s - \frac{2k^2\hat{q}(0)}{M^2} p_+ \int_0^t \frac{p_-(s)}{K^2(s)W(s)}\,\mathrm{d}s, \tag{4.1}$$

where $p_\pm$ are solutions to the homogeneous equation (3.5) and

$$W = p_+ \frac{\mathrm{d}p_-}{\mathrm{d}t} - p_- \frac{\mathrm{d}p_+}{\mathrm{d}t},$$

is the corresponding Wronskian. This interaction can lead to acoustic wave excitation by the aperiodic vorticity perturbations as already found by Chagelishvili *et al.* (1997*b*), so we can write (4.1) in terms of a vorticity and an acoustic wave component: $\hat{p}_{part}(t) = \hat{p}_{vort}(t) + \hat{p}_{wave}(t)$. In this section, we will use exponential–asymptotic techniques to analytically estimate the amplitude of the generated acoustic waves. There are two regimes depending on M/k that are separated by the corresponding coupling strength between vorticity dynamics and acoustic waves, and we will study them separately.

4.1. *Weak coupling ($M/k \ll 1$)*

The vorticity component, $\hat{p}_{vort}(t)$, can be isolated by taking the incompressible limit ($M \to 0$). If we choose initial conditions such that the time derivatives are initially bounded as $M \to 0$, then they are bounded for all times (Kreiss *et al.* 1991). The solution then converges to the incompressible solution as $M \to 0$ (Kreiss *et al.* 1991), for which the acoustic waves are absent for all times. In this case, (4.1) reduces to the incompressible solution (2.12) in which the time-dependent Fourier pressure amplitude is given by

$$\hat{p}(t) = \hat{p}_{vort}(t) = \hat{p}_{M0}(t) = \frac{2k^2\hat{q}(0)}{(k^2 + (m - kt)^2)^2}. \tag{4.2}$$

The velocity field is non-divergent, and the resulting vorticity perturbations are non-propagating. Moreover, the cross-stream component of vorticity of these perturbations is conserved, leading to perturbation velocity growth as discussed in § 2.2. For $M \neq 0$, compressibility produces a mixing of vortical and divergent motion associated with acoustic waves. As a result, the initial perturbations will also project on the acoustic wave manifold. A rough first-order estimate of the amount of initial energy radiated away as acoustic waves is given by calculating the projection of the non-divergent initial conditions $[\hat{u}(0), \hat{v}(0), \hat{p}(0)] = [-m/k, 1, 2ik/(k^2 + m^2)]$, on the acoustic wave manifold. Since in this regime we have weak compressibility ($M/k \ll 1$), we expect to leading order a behaviour similar to the incompressible limit, and we therefore seek a solution for the vorticity waves of the form

$$\hat{p}_{vort}(t) = p_0(t) + M^2 p_1(t) + \cdots, \tag{4.3}$$

where $p_0(t) = \hat{p}_{M0}(t)$ corresponds to the $M = 0$ solution that is given by (4.2) and a similar expansion in powers of M for $\hat{p}_{wave}$. Since for $M/k \ll 1$, $p_\pm$ is given by (3.6)

and is a rapidly oscillating function, such an expansion can be easily obtained using integration by parts in (4.1),

$$\int_0^t \frac{p_\pm(s)}{W(s)K^2(s)}\,\mathrm{d}s = \frac{\mathrm{i}M}{2}\int_0^t \mathrm{e}^{\pm(\mathrm{i}/M)\int_0^s K(\tau)\,\mathrm{d}\tau}\frac{\sqrt{K(s)}}{(k^2+(m-ks)^2)^2}\,\mathrm{d}s$$
$$= \frac{\pm M^2\mathrm{e}^{\pm(\mathrm{i}/M)\int_0^t K(s)\,\mathrm{d}s}}{2(k^2+(m-kt)^2)^2\sqrt{K(t)}} \mp \frac{M^2}{2(k^2+m^2)^2\sqrt{k^2+m^2}} + O(M^3),$$

yielding to leading order the particular solution

$$p_{part}(t) = \frac{2k^2\hat{q}(0)}{(k^2+(m-kt)^2)^2} - \frac{k^2\hat{q}(0)\sqrt{K(t)}}{(k^2+m^2)^2\sqrt{K(0)}}\left(\mathrm{e}^{(\mathrm{i}/M)\int_0^t K(s)\,\mathrm{d}s} + \mathrm{e}^{(-\mathrm{i}/M)\int_0^t K(s)\,\mathrm{d}s}\right)$$

and the solution to (2.8),

$$\hat{p}(t) = \hat{p}_{vort} + \hat{p}_{wave} = \frac{2k^2\hat{q}(0)}{(k^2+(m-kt)^2)^2} - \frac{4\mathrm{i}k^3M^2}{(k^2+m^2)^3\sqrt{K(0)}}\sqrt{K(t)}\cos\left(\frac{1}{M}\int_0^t K(s)\,\mathrm{d}s\right). \tag{4.4}$$

The last term in (4.4) corresponds to the propagating acoustic waves studied in § 3.2, having an amplitude $O(M^2/k^2)$. Projection of non-divergent initial conditions on to propagating acoustic waves is therefore very weak.

The following question then arises: if we carefully chose initial conditions with minimal projection on the acoustic wave manifold, would the initial energy remain in the non-propagating vorticity wave for all times? If this were true, $\hat{p}_{wave}$ would be zero for all times, and the solution would be given by (4.3). However, expansion (4.3) is asymptotic rather than convergent as a result of exponentially small terms that it can not capture. We show in Appendix B that these terms represent propagating acoustic waves excited abruptly at time $t = m/k$. As in the case of gravity wave generation by sheared disturbances in a stratified horizontal shear flow (Bakas & Farrell 2009) and on the f-plane (Vanneste & Yavneh 2004), spontaneous generation of acoustic waves can be analysed as an instance of a Stokes phenomenon (Olver 1974) in which the subdominant solution (waves) is switched on by the dominant solution (vorticity perturbation) when time crosses a Stokes line. To determine the leading-order approximation to the acoustic wave amplitude, we consider oscillation-free initial conditions. That is we choose $[\hat{p}(0), \mathrm{d}\hat{p}/\mathrm{d}t|_{t=0}] = [\hat{p}_{M0}(0), \mathrm{d}\hat{p}_{M0}/\mathrm{d}t|_{t=0}]$ such that the projection of the initial conditions on the acoustic waves is $O(M^2m^{-4})$. By choosing m appropriately, we can therefore make the second term in (4.4) approach zero with arbitrary precision. We then use in Appendix B asymptotic matching in the complex t-plane (Hakim 1998) to show that the solution at large times is given by

$$\hat{p}(t) = \hat{p}_{vort}(t) + \frac{\hat{q}(0)\sqrt{2\pi}\mathrm{e}^{-k\pi/4M}\sqrt{K(t)}}{kM^{3/2}}\left(\mathrm{e}^{(\mathrm{i}/M)\int_0^t K(s)\,\mathrm{d}s} + \mathrm{e}^{(-\mathrm{i}/M)\int_0^t K(s)\,\mathrm{d}s}\right), \tag{4.5}$$

where ϕ_0 is given by (B 3). These spontaneously generated acoustic waves are exponentially small for small Mach numbers, being $O(M^{-3/2}\mathrm{e}^{-k\pi/4M})$. As a result, the large energy gained by the vorticity perturbation for $t < m/k$ (see § 2.2) is transferred back to the mean flow. This analytic result was confirmed by numerically solving (2.8) and then estimating the acoustic wave amplitude for large times T through the equation

$$A_s = \frac{1}{2\sqrt{K(T)}}\left[(\hat{p}(T)-\hat{p}_{M0}(T))^2 + \frac{M^2}{K(T)^2}\left(\frac{\mathrm{d}\hat{p}}{\mathrm{d}t}|_{t=T} - \frac{\mathrm{d}\hat{p}_{M0}}{\mathrm{d}t}|_{t=T}\right)^2\right]^{1/2}. \tag{4.6}$$

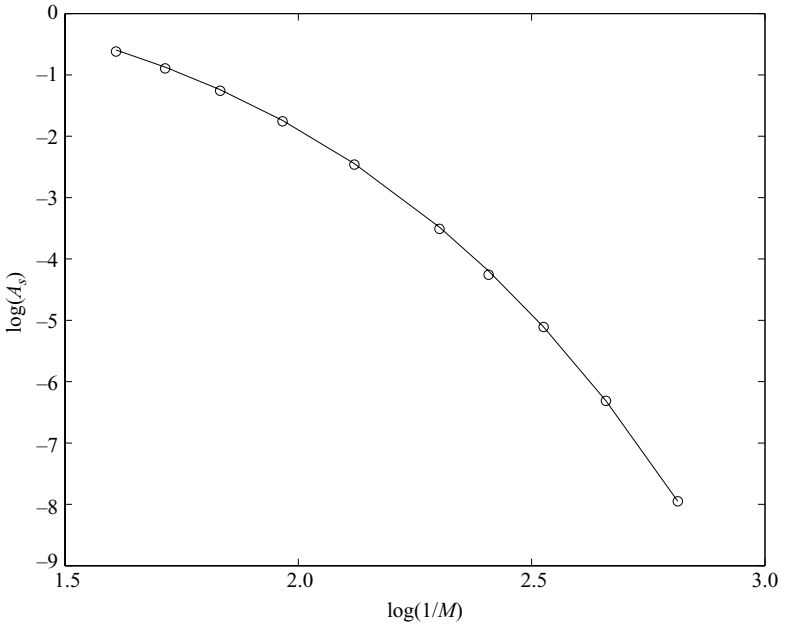

FIGURE 5. Amplitude of the spontaneously generated acoustic wave A_s as a function of $1/M$. The analytic estimate given by (4.5) is shown by the solid line, and the numerically calculated estimate given by (4.6) is shown by the open circles. The wavenumbers are $(k, m) = (1, 10)$, and the oscillation-free initial conditions are such that $\hat{q}(0) = 1$.

Figure 5 shows A_s as a function of M along with the analytic result revealing an excellent agreement even for moderate values of M. In summary, for $M/k \ll 1$, projection of the initial conditions on the acoustic wave manifold is weak, with the amplitude of the acoustic waves being $O(M^2/k^2)$ for non-divergent initial conditions. But even in the case of oscillation-free initial conditions, acoustic waves are inevitably excited by vorticity perturbations with an exponentially small amplitude in k/M.

4.2. *Strong coupling (M/k $O(1)$)*

In this strong-coupling regime, both the projection of the initial conditions on the acoustic waves and the amplitude of the spontaneously generated acoustic waves is of order one. This is illustrated in figure 6, where the evolution of $\hat{p}_{wave}(t)$ with time for $m/k = 5$ is shown. The forced waves' amplitudes remain at very low values until time $t = m/k = 5$. At that time, the large energy amplification of the non-propagating vorticity perturbations due to the Orr mechanism discussed in § 2.2 is transferred to the spontaneously generated acoustic waves causing the amplitude of these forced waves to increase rapidly and to reach very large values as illustrated in figure 6. The amplitude of the forced waves is numerically calculated using (4.6) and is plotted as a function of the Mach number in figure 7. For M/k $O(1)$, the amplitude of the forced waves is of order $\hat{q}(0)M^{-3/2}$, showing that a large initial vorticity perturbation can lead to substantial excitation of waves that can then further grow in the manner discussed in the previous section. For large Mach numbers the amplitude decreases rapidly as M^{-2}, and wave excitation is not very efficient. The efficiency of wave excitation by vorticity perturbations and its contribution to perturbation energy growth will now be further investigated by performing optimization calculations.

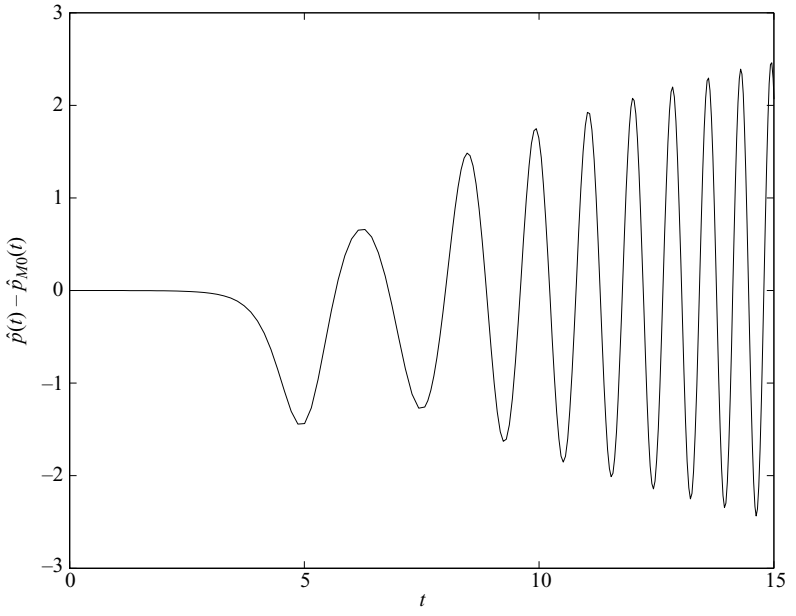

FIGURE 6. Evolution of the pressure field of the spontaneously generated acoustic waves $\hat{p}_{wave}(t) = \hat{p}(t) - \hat{p}_{M0}(t)$ for $(k, m) = (1, 5)$. The Mach number is $M = 1$, and the oscillation-free initial conditions are such that $\hat{q}(0) = 1$.

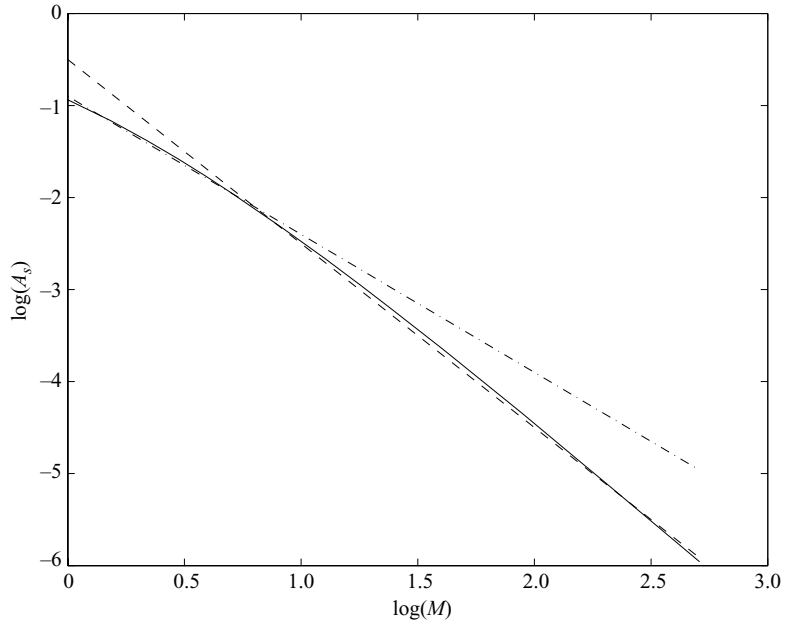

FIGURE 7. Amplitude of the spontaneously generated acoustic wave A_s as a function of M. Lines for $M^{-3/2}$ (dash-dotted line) and M^{-2} (dashed line) are also shown. The wavenumbers are $(k, m) = (1, 10)$, and the oscillation-free initial conditions are such that $\hat{q}(0) = 1$.

5. Optimals

As discussed in the previous sections, the synergy between the lift-up mechanism, and the downgradient irrotational and solenoidal part of the Reynolds stress along with efficient wave excitation by vorticity perturbations leads to energy amplification of plane wave perturbations. In order to obtain an upper bound for the transient growth, we calculate in this section the initial conditions yielding the largest energy growth over a specified time interval T_{opt}. Similar optimization calculations performed by Farrell & Ioannou (2000) for large Mach numbers showed that viscocity has a significant impact on perturbation growth. Therefore, to include viscous effects, optimization calculations in this section are performed for a viscous flow as well but for a large range of Mach numbers. A complete analysis proceeds from first using the viscous equations for compressible sheared waves (Farrell & Ioannou 2000):

$$\frac{\mathrm{d}\hat{u}}{\mathrm{d}t} = -\mathrm{i}k\hat{p} - \frac{1}{Re}\left(K^2(t) + \frac{k^2}{3}\right)\hat{u} - \left(1 + \frac{k(m-kt)}{3Re}\right)\hat{v}, \tag{5.1}$$

$$\frac{\mathrm{d}\hat{v}}{\mathrm{d}t} = -\mathrm{i}(m-kt)\hat{p} - \frac{k(m-kt)}{3Re}\hat{u} - \frac{1}{Re}\left(K^2(t) + \frac{(m-kt)^2}{3}\right)\hat{v}, \tag{5.2}$$

where the Reynolds number is defined as $Re = L^2\alpha/\nu$ in which ν is the coefficient of shear viscosity and pressure evolves according to (2.6). Since for an unbounded shear flow there is no intrinsic space scale, the Reynolds number is prescribed for a given coefficient of viscosity on perturbations having unit zonal wavenumber ($k = 1$). Perturbations with larger zonal scale can be interpreted as evolving in a flow with a correspondingly higher Reynolds number.

Equations (2.6), (5.1) and (5.2) can then be written in the compact form:

$$\frac{\mathrm{d}\boldsymbol{\chi}}{\mathrm{d}t} = \boldsymbol{A}(t)\boldsymbol{\chi},$$

where $\boldsymbol{\chi}$ is the column vector, $\boldsymbol{\chi} = [\hat{u}, \hat{v}, M\hat{p}]^T$, and $\boldsymbol{A}(t)$ is

$$\boldsymbol{A}(t) = \begin{pmatrix} -(K^2(t) + k^2/3)/Re & -1 - k(m-kt)/(3Re) & -\mathrm{i}k/M \\ -k(m-kt)/(3Re) & -(K^2(t) + (m-kt)^2/3)/Re & -\mathrm{i}(m-kt)/M \\ -\mathrm{i}k/M & -\mathrm{i}(m-kt)/M & 0. \end{pmatrix}$$

For a given wavenumber m, singular value decomposition of the finite-time propagator

$$\Phi(t) = \lim_{N\to\infty} \prod_{n=1}^{N} \mathrm{e}^{\boldsymbol{A}(nt/N)t/N},$$

mapping the initial perturbation to its state at time t ($\boldsymbol{\chi}(t) = \Phi(t)\boldsymbol{\chi}(0)$), identifies the optimal initial conditions and the corresponding growth $E^m_{opt}(T_{opt})$ (Farrell 1988; Reddy & Henningson 1993; Farrell & Ioannou 1996). The perturbation growing the most is then obtained by numerically determining the wavenumber m maximizing $E^m_{opt}(T_{opt})$, and the corresponding growth is $E_{max} = \max_m(E^m_{opt}(T_{opt}))$.

The optimal growth E_{max} as a function of the optimizing time T_{opt} is shown in figure 8 for Mach numbers $M = 1$ and $M = 50$. While the $M = 1$ case is typical of engineering applications, highly supersonic flows in which $M = 50$ can be found in thin, Keplerian astrophysical disks in which also a polytropic fluid is typically considered (Pringle 1981; Papaloizou & Lin 1995). Large and robust growth is found for both values of Mach number even in this case of unbounded flow in which no unstable modes are supported, but different mechanisms dominate the growth in these two cases.

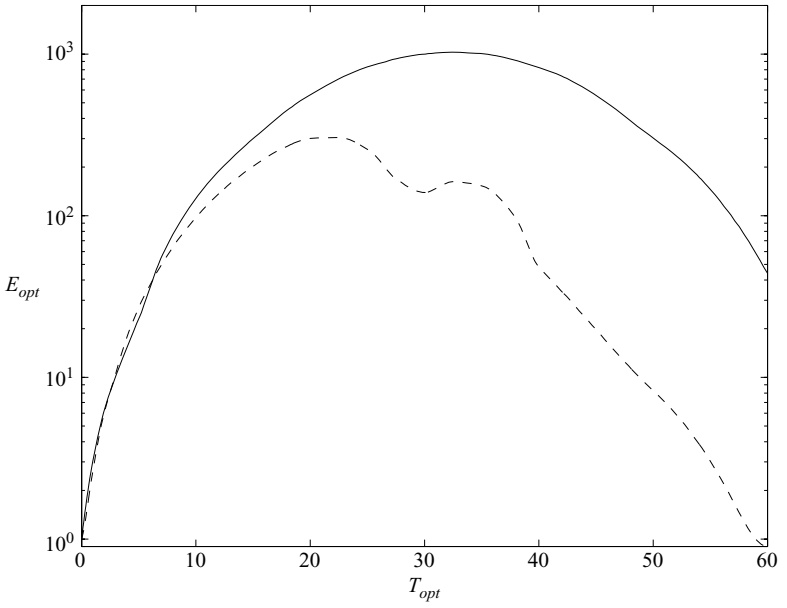

FIGURE 8. Optimal energy growth E_{max} achieved at T_{opt} as a function of the optimization time T_{opt} for Mach numbers $M = 1$ (solid line) and $M = 50$ (dashed line). The Reynolds number is $Re = 5000$.

For $M = 1$ and small optimizing times, the optimal perturbations have an initial tilt $m/k \sim T_{opt}$ such that the plane wave assumes a cross-stream orientation ($m - kt = 0$) at a time $t \sim T_{opt}$, maximizing the benefit from transient amplification of cross-stream velocity of vorticity perturbations. For larger optimizing times, $m/k \sim T_{opt}/2$ such that amplification of vorticity perturbations due to the Orr mechanism occurs early, enabling the effective transfer of energy to acoustic waves and allowing enough time for the acoustic waves to grow through the downgradient irrotational part of the Reynolds stress. This three-stage process of vorticity wave amplification, energy transfer to acoustic waves and acoustic wave amplification is illustrated in figure 9(a), where the evolution of each component of the Reynolds stress ($\overline{uv}_{Orr}$, $\overline{uv}_{com}$, $\overline{uv}_{lift}$ and $\overline{uv}_{interf}$) is shown. Initially $\overline{uv}_{Orr}$ is the dominant energy source peaking right before $t_v = m/k = 12$. After the excitation of acoustic waves at t_v, $\overline{uv}_{comp}$ becomes the dominant energy source for the generated acoustic waves, while the Orr mechanism becomes an energy sink for the vorticity perturbations. The contribution of the lift-up mechanism in perturbation growth is small in this case, as despite the fact that $\overline{uv}_{lift}$ has approximately the same amplitude as $\overline{uv}_{Orr}$, it oscillates rapidly around zero and averages to a small total amount.

To address the sensitivity of the attained growth to the viscous damping rate, we performed optimization calculations varying the Reynolds number. As shown in figure 10(a) the optimization time at which the maximum optimal growth is attained is $O(Re^{1/3})$, consistent with the e-folding time $O(Re^{1/3})$ of vorticity dynamics for an incompressible flow (Bakas, Ioannou & Kefaliakos 2001). However, the global optimal growth that is $O(Re)$ as illustrated in figure 10(b) is larger by a factor of $Re^{1/3}$ compared to the corresponding growth for an incompressible flow.

For $M = 50$ the mechanism of acoustic wave excitation from vorticity waves is inefficient, as the generated acoustic wave amplitude is $O(M^{-2})$. The optimal

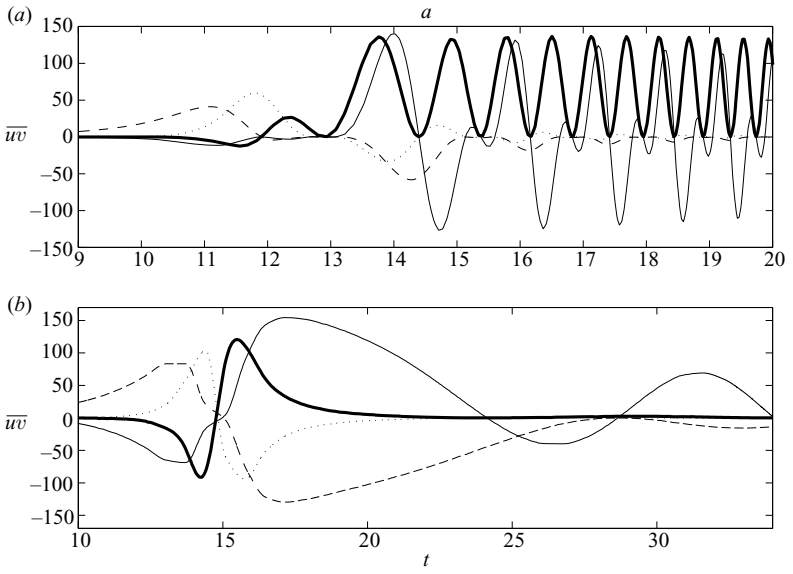

FIGURE 9. (*a*) Evolution of the irrotational component $\overline{uv}_{comp}$ (thick solid line), the advection component $\overline{uv}_{lift}$ (solid line), the solenoidal component $\overline{uv}_{Orr}$ (dashed line) and interference component $\overline{uv}_{interf}$ (dotted line) of the Reynolds stress for the plane wave with $(k, m) = (1, 12)$ and initial conditions $(\hat{u}(0), \hat{v}(0), \hat{p}(0)) = (1, -0.1, -11\mathrm{i})$. The Reynolds number is $Re = 5000$, and the initial plane wave leads to the largest energy growth at $T_{opt} = 20$ for $M = 1$. (*b*) The same as (*a*) for the optimal plane wave with $(k, m) = (1, 15)$ and initial conditions $(\hat{u}(0), \hat{v}(0), \hat{p}(0)) = (1, -1.1, -0.14\mathrm{i})$ that leads to the largest energy growth at $T_{opt} = 20$ for $M = 50$.

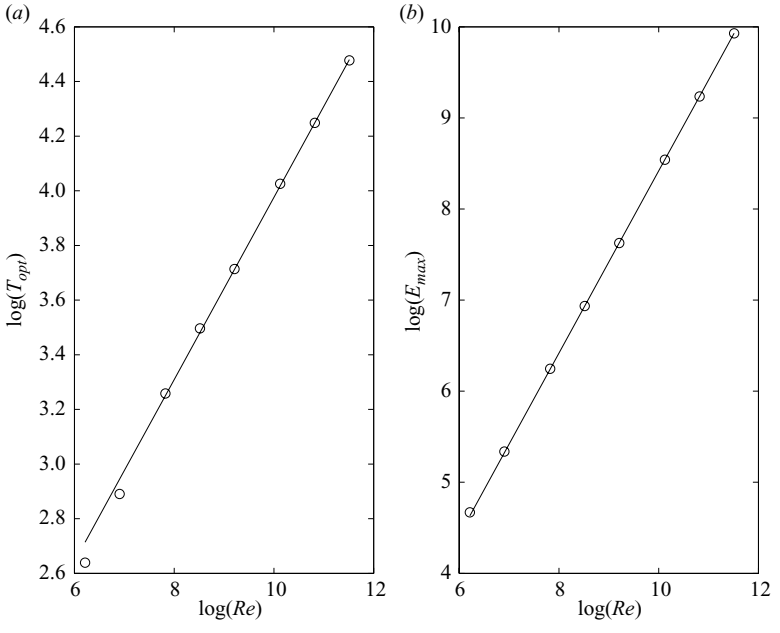

FIGURE 10. (*a*) Optimization time at which the maximum optimal growth is attained for each Reynolds number (open circles) as a function of Reynolds number. A straight line with slope 1/3 is also plotted for reference. (*b*) Maximum optimal energy growth E_{max} achieved at each Reynolds number (open circles) as a function of the Reynolds number. A straight line with slope 1 is also plotted for reference. The Mach number is $M = 1$.

	$M/k \ll 1$	$M/k\ O(1)$	$M/k \gg 1$
Characteristics of growth	Two-stage process: (i) Growth of vorticity perturbations due to $\overline{uv}_{Orr}$ (ii) Weak acoustic wave excitation	Three-stage process: (i) Growth of vorticity perturbations due to $\overline{uv}_{Orr}$ (ii) Efficient acoustic wave excitation (iii) Growth of acoustic waves due to $\overline{uv}_{comp}$	Two-stage process: (i) Growth of cross-stream velocity perturbations due to $\overline{uv}_{Orr}$ (ii) Initiation of lift-up mechanism
Maximum growth	$O(Re^{2/3})$	$O(Re)$	Increasing with Re but does not follow a power law
Growth of	Kinetic energy	Kinetic and potential energy	Streamwise velocity

TABLE 1. Characteristics of transient growth mechanisms.

perturbations therefore utilize the synergy between the downgradient solenoidal component of the Reynolds stress and the lift-up mechanism studied in § 3.3, which leads to robust growth of the streamwise velocity of acoustic waves. As shown in figure 9(*b*), where the evolution of each component of the Reynolds stress is plotted for $T_{opt} = 20$, the initial contribution of $\overline{uv}_{Orr}$ is significant and leads to an increase in the cross-stream velocity and to a large advection of u in the cross-stream direction. This large advection utilizes the lift-up mechanism that becomes the dominant energy source after $t = m/k = 15$ (see figure 9*b*) and leads to a significant growth of streamwise velocity comprising about 90 % of the energy amplification in this case. For smaller optimization times, the optimal perturbations have an initial tilt $m/k \lesssim T_{opt}$ such that the initiation of the lift-up mechanism occurs right before the optimization time, whereas for $T_{opt} \geqslant 30$ the initiation of the lift-up mechanism occurs early at approximately the same time as for $T_{opt} = 20$ shown in figure 9(*b*). That is instead of having a large initial m/k so that the boost from the lift-up mechanism occurs before the optimization time, it is energetically more efficient for the optimal perturbations to have a rather low m/k (that is attenuated less by diffusion) such that there is a large initial energy growth followed by a secondary growth at about the optimization time that is associated with the secondary peak of $\overline{uv}_{lift}$ (see figure 9*b*). This exploitation of the secondary peak of $\overline{uv}_{lift}$ by the optimal perturbations is also underlying the secondary peak of optimal growth with T_{opt} shown in figure 8 for $M = 50$. Finally it is worth noting that even though the optimal growth increases with the Reynolds number (not shown) it does not follow a power law like the $M = 1$ case.

In summary, there are three distinct regimes of transient growth with characteristics summarized in table 1: in weakly compressible flows vorticity perturbations grow in a manner similar to incompressible flows with a weak excitation of acoustic waves. In subsonic and sonic flows, the mechanism of acoustic wave excitation by vorticity perturbations is dominant due to the strong coupling between vorticity perturbations and acoustic waves for Mach numbers $M\ O(k)$. On the other hand, supersonic flows and highly supersonic flows favour streamwise velocity growth, taking advantage of the strength of the lift-up mechanism in this case. For small optimizing times, both processes lead to comparable transient growth, while for larger optimizing times, the process of acoustic wave excitation and growth leads to larger transient energy growth

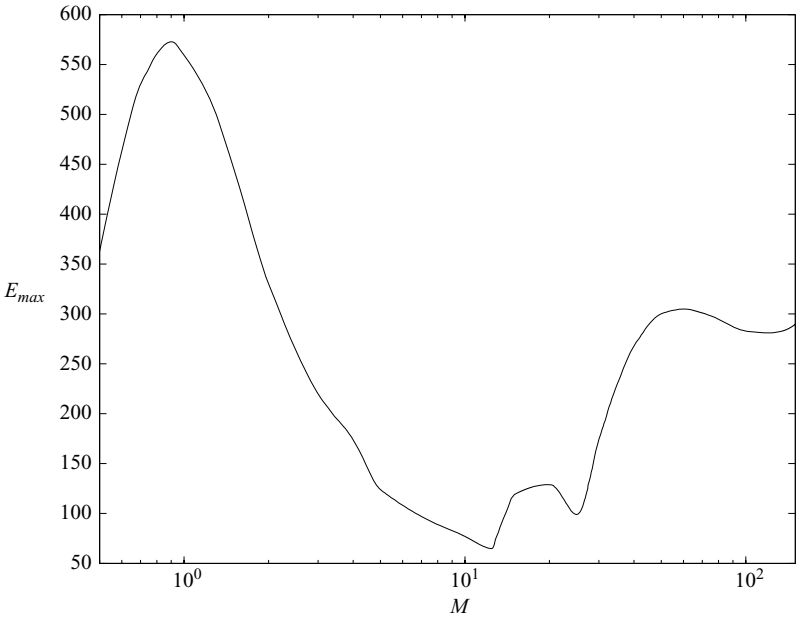

FIGURE 11. Optimal energy growth E_{max} achieved at $T_{opt} = 20$ as a function of the Mach number. The Reynolds number is $Re = 5000$.

as illustrated in figure 11 showing the optimal growth at $T_{opt} = 20$ as a function of the Mach number.

6. Discussion

We now relate the results obtained in this work to previous theoretical studies of compressible, constant-shear flows utilizing the convected coordinate formulation and addressing different aspects of perturbation growth. Chagelishvili *et al.* (1994, 1997*a*) were the first to address adiabatic growth of acoustic waves in the absence of aperiodic vorticity perturbations by providing asymptotic solutions. For moderate Mach numbers, Chagelishvili *et al.* (1997*a*) found that acoustic energy growth can be larger compared to the adiabatic regime and suggested that the lift-up mechanism plays a role in the observed growth. This argument was tested in this study, where the role of the lift-up mechanism was clarified and the synergy between the lift-up mechanism and the solenoidal part of the Reynolds stress was clearly shown to be underlying the observed excess growth of planar perturbations. It is also worth noting that agreement of our results in terms of energy growth of planar perturbations to the findings of Chagelishvili *et al.* (1997*a*) for three-dimensional acoustic waves shows that most of the characteristics of the evolution of planar acoustic waves remain unaltered in three dimensions, suggesting that the growth mechanisms in three dimensions are captured by our two-dimensional analysis. However, a careful investigation of perturbation evolution in three dimensions as well as optimization calculations are needed to validate this conclusion.

Moreover, Chagelishvili *et al.* (1997*b*) studied the abrupt acoustic wave excitation process by the aperiodic vorticity perturbations in the moderate-Mach-number regime, using numerical integration of the equations. In this study, the numerical evidence of Chagelishvili *et al.* (1997*b*) is complemented by asymptotic estimates for the

amplitude of the generated acoustic waves through the use of exponential–asymptotic techniques. The analytic treatment offers the advantage of giving a precise description of acoustic wave generation in a simple model flow, as it unambiguously separates the aperiodic vorticity perturbations from the propagating acoustic waves. A systematic investigation of the conditions favouring an efficient wave excitation was also pursued in this study by calculating the initial conditions producing optimal growth over a specified time interval.

On the other hand, Farrell & Ioannou (2000) addressed perturbation evolution for a viscous flow in the large-Mach-number limit and distinguished two phases of growth: an early-time growth due to the solenoidal component of the Reynolds stress that is initially downgradient for perturbations with constant-phase lines tilted against the shear and a subsequent growth due to the irrotational component of the Reynolds stress that is downgradient for large times. Farrell & Ioannou (2000) however found based on numerical integrated solutions that the late-time growth is not sustained, as the perturbations' length scale constantly decreases leading to increased viscous damping. Farrell & Ioannou (2000) also concluded that the Reynolds stress associated with the interactions between the solenoidal and the irrotational velocity fields, which was termed $\overline{uv}_{lift}$ in this study, does not play a significant role in perturbation growth for large times. In this study, we found that even though the contribution of the lift-up mechanism in perturbation growth is small in the $t \to \infty$ limit in agreement with Farrell & Ioannou (2000), its synergy with the solenoidal component of the Reynolds stress occurring within the first few advective time units accounts for most of the observed transient growth at finite times. In terms of the effect of viscosity on perturbation growth, optimization calculations performed in this study for a wide range of Mach numbers and Reynolds numbers confirmed the conclusion of Farrell & Ioannou (2000) that was reached for large Mach numbers only, that the transient growth is not sustained for large times for which the major contribution comes from $\overline{uv}_{comp}$, as the total wavenumber of these growing disturbances also increases linearly with time, resulting in an accelerating viscous damping rate.

7. Conclusions

Non-modal mechanisms underlying transient growth of acoustic and vorticity wave perturbations in an unbounded compressible shear flow were investigated making use of closed form solutions. Propagating acoustic waves amplify mainly due to two mechanisms that are exemplified by considering two separate limits. In the limit of streamwise-independent perturbations ($k = 0$), acoustic waves were found to grow due to advection of streamwise velocity to regions of higher/lower background velocity. This growth mechanism that is often referred to as the lift-up effect (Ellingsen & Palm 1975; Reddy & Henningson 1993) results in an amplification of streamwise velocity that was found to be increasing with the vertical wavelength of perturbations and with Mach number and for $M/m \gg 1$ leads to an almost linear increase in streamwise velocity with time. In the limit of weakly compressible flows ($M/k \ll 1$), acoustic waves amplify when their phase lines are tilted with the shear due to the kinetic energy source associated with the downgradient irrotational component of the Reynolds stress. The energy of the acoustic waves grows linearly for large times with the largest growth achieved for waves with phase lines initially tilted almost vertically (Chagelishvili *et al.* 1997*a*; Farrell & Ioannou 2000).

The role of each of these mechanisms as well as the downgradient solenoidal component of the Reynolds stress in acoustic wave growth for M/k $O(1)$ was

investigated, and the interplay between the three mechanisms was found to produce large and robust energy amplification. Acoustic waves with phase lines tilted against the shear ($m/k > 0$) were found to benefit more from this synergy compared to opposite tilted waves. For larger Mach numbers, the lift-up mechanism dominates, and streamwise velocity of acoustic waves is significantly amplified leading to large streamwise streaks within the waves and potentially to shear instability.

On the other hand, non-propagating vorticity perturbations coexisting with the propagating acoustic waves amplify due to kinematic deformation of vorticity by the mean flow, a growth mechanism that is typically found in incompressible shear flows and is often referred to as the Orr mechanism (Orr 1907). For weakly compressible flows ($M/k \ll 1$), a weak coupling between vorticity perturbations and acoustic waves was found using exponential–asymptotic techniques. In the case of oscillation-free initial conditions, while for $t < m/k$ the energy evolution is dominated by the vorticity wave dynamics, two counter-propagating acoustic waves with an exponentially small amplitude $O(\exp(-k\pi/4M))$ are spontaneously generated at $t \sim m/k$ through a Stokes phenomenon. For M/k $O(1)$, a strong coupling was found with the energy gained by vorticity perturbations being transferred to acoustic waves that finally emerge with an amplitude of order $\hat{q}(0)M^{-3/2}$.

In order to quantify the potential for perturbation growth due to the synergy of the various growth mechanisms including acoustic wave excitation by non-propagating vorticity perturbations, the optimally growing perturbations over a specified time interval were calculated in the case of a viscous flow. For M $O(k)$, acoustic wave excitation by vorticity perturbations and the subsequent growth of the acoustic waves due to the downgradient irrotational component of the Reynolds stress were found to lead to robust energy growth $O(Re)$ that is equipartitioned between potential and kinetic forms. Furthermore, the attained growth is larger than the corresponding growth in incompressible flows by a factor of $Re^{1/3}$. For larger Mach numbers, the wave excitation mechanism is not effective, and the synergy between the lift-up mechanism and the downgradient solenoidal component of the Reynolds stress was found to dominate the growth and to lead to a large amplification of streamwise velocity.

Even though the unbounded flow considered in this study is an idealized flow permitting closed form solutions, the transient growth mechanisms that were investigated and their synergy are expected to play a significant role in the dynamics of realistic bounded flows as well. In the case of reflecting boundaries, the possibility of continuous over-reflection of the acoustic waves arises, as these propagating waves can grow transiently in the manner described in this study while being continuously reflected at the boundaries. This over-reflection process has been invoked in previous studies to explain the instability of compressible flows (Hu & Zhong 1998) and of plane parallel shear flows (Lindzen 1988), but the role of transient growth in this process has not been investigated. Identification of the unstable modes found by Farrell & Ioannou (2000) in their study of a bounded polytropic fluid with over-reflecting acoustic waves and investigation of the role of transient growth in this process is the subject of current research efforts and will be reported in a future study. In addition to the influence of the boundaries, the influence of the thermodynamic properties of the flow on the dynamics is under current investigation. Nonetheless, we can already remark that comparison of our results to the findings of previous studies of non-modal perturbation growth in a compressible boundary layer (Hanifi *et al.* 1996) and in a perfect gas model (Malik *et al.* 2006) reveals that although some of the characteristics of the lift-up mechanism are influenced by the choice of gas properties,

the lift-up mechanism plays an important role in perturbation growth regardless of the thermodynamics of the flow.

Finally, it is worth noting that the mechanism of acoustic wave generation examined in this study appears to be underlying wave excitation in more complicated flows as well, as shown by the numerical studies of Mamatsashvili & Chagelishvili (2007) and Tevzadze *et al.* (2008). In view of the advantage of the exponential–asymptotic approach to allow for a transparent separation of the acoustic waves from the non-propagating vortical motions and to also allow an analytic estimate of the wave amplitude, in the future we plan on applying the exponential–asymptotic techniques to a broader class of flows.

The author would like to thank Professor Petros Ioannou for stimulating discussions and three anonymous reviewers for their useful comments and numerous suggestions, which helped to improve the manuscript. This research was supported by an IKY grant.

Appendix A. Optimal streamwise-independent perturbations

The streamwise-independent perturbations leading to the largest energy growth over a specified time interval within the initial stage of wave interference are obtained by following the method outlined in § 5. A complete analysis proceeds from first using (2.7) (for $\hat{q}(0) = 0$) to express $\hat{u}$ in terms of $\hat{p}$ and then writing (2.4)–(2.6) in the compact form:

$$\frac{\mathrm{d}\boldsymbol{\chi}_0}{\mathrm{d}t} = \boldsymbol{B}(t)\boldsymbol{\chi}_0, \tag{A 1}$$

where $\boldsymbol{\chi}_0$ is the column vector, $\boldsymbol{\chi}_0 = [\hat{v}, \hat{p}]^T$, and $\boldsymbol{B}(t)$ is

$$\boldsymbol{B} = -\mathrm{i}m \begin{pmatrix} 0 & 1 \\ 1/M^2 & 0. \end{pmatrix}$$

We then express (A 1) in terms of the new variable $\boldsymbol{y} = \boldsymbol{M}_{k0}^{1/2}\boldsymbol{\chi}_0$, where $\boldsymbol{M}_{k0}$ is the energy metric,

$$\boldsymbol{M}_{k0} = \frac{1}{4}\begin{pmatrix} 1 & 0 \\ 0 & M^2(1 + M^2/m^2), \end{pmatrix}$$

for which perturbation energy is given by the inner product: $E = \boldsymbol{y}^\dagger \boldsymbol{y}$. In this variable the governing equations are transformed to

$$\frac{\mathrm{d}\boldsymbol{y}}{\mathrm{d}t} = \boldsymbol{D}_0 \boldsymbol{y}, \tag{A 2}$$

where $\boldsymbol{D}_0$ is

$$\boldsymbol{D}_0 = \boldsymbol{M}_{k0}^{1/2}\boldsymbol{B}\boldsymbol{D}_{k0}^{-1/2} = \begin{pmatrix} 0 & -\mathrm{i}\omega_0^2/\sqrt{1+\omega_0^2} \\ -\mathrm{i}\sqrt{1+\omega_0^2} & 0, \end{pmatrix}$$

and ω_0 is given by (3.4). The solution of (A 2) is $\boldsymbol{y}(t) = e^{\boldsymbol{D}_0 t}\boldsymbol{y}(0)$, where

$$e^{\boldsymbol{D}_0 t} = \begin{pmatrix} \cos(\omega_0 t) & -\dfrac{\mathrm{i}\omega_0}{\sqrt{1+\omega_0^2}}\sin(\omega_0 t) \\ -\dfrac{\mathrm{i}\sqrt{1+\omega_0^2}}{\omega_0}\sin(\omega_0 t) & \cos(\omega_0 t) \end{pmatrix}$$

is the propagator. The initial perturbation leading to the largest energy growth E^m_{opt} over a specified time interval $t = T_{opt}$ for a given wavenumber m can be identified as the eigenvector corresponding to the largest eigenvalue of $\boldsymbol{P} = e^{\boldsymbol{D}_0{}^\dagger T_{opt}} e^{\boldsymbol{D}_0 T_{opt}}$ (Farrell 1988; Reddy & Henningson 1993; Farrell & Ioannou 1996). The optimal perturbation can be then found by maximizing E^m_{opt} over the vertical wavenumber m. Eigenanalysis of $\boldsymbol{P}$ reveals that the largest eigenvalue for all wavenumbers m, corresponding to the optimal growth is $\sigma = 1 + T^2_{opt}$ and is achieved for non-propagating perturbations having $m = 0$. However for $\omega_0 T_{opt} \ll 1$, the optimal growth is very close to this value: $\sigma = 1 + T^2_{opt} + O(\omega_0^2 T^2_{opt})$. Therefore the propagating optimal perturbations have large vertical wavelengths and are cross-stream velocity perturbations as $(\hat{u}(0), \hat{p}(0))$ $O(m/M) \ll 1$.

Appendix B. Analysis of the generation of exponentially small acoustic waves as a Stokes phenomenon

Bakas & Farrell (2009) found in their study of the interaction between vortical perturbations and gravity waves in a stratified horizontal shear flow that gravity waves were spontaneously generated by oscillation-free initial conditions. They also found that the spontaneous wave generation can be analysed as a Stokes phenomenon (Olver 1974; Berry 1989) in which the subdominant homogeneous solution is abruptly 'turned on' by the dominant, inhomogeneous solution when time, t, crosses a Stokes line arising from singularities of the asymptotic expansion of the solution in the complex t-plane. We follow the analyses in Vanneste & Yavneh (2004) and Bakas & Farrell (2009) to address this possibility in our case as well and analyse the asymptotic expansion (4.3) near its singularities in the complex t-plane at $t_\pm = m/k \pm \mathrm{i}$ that coincide with the singularities of the homogeneous solution. The Stokes lines, defined as the asymptotes of the curves $\mathrm{Im} \int K(s)\, \mathrm{d}s = 0$ as $t \to t_\pm$, are tangent to

$$S_1, \arg(t - t_\pm) = \mp\frac{5\pi}{6}, \quad S_2, \arg(t - t_\pm) = \mp\frac{\pi}{6}, \quad S_3, \arg(t - t_\pm) = \mp\frac{\pi}{2},$$

as close to $t_\pm$, $K = \sqrt{k^2 + (m - kt)^2} \simeq \sqrt{2} k \mathrm{e}^{\pm \mathrm{i}\pi/4} (t - t_\pm)^{1/2}$. In the real-time axis, S_3 is crossed when time takes the value m/k, and as a result we expect the spontaneous generation of acoustic waves through a Stokes phenomenon.

The amplitude of the generated waves can be found by integration of (2.8) on a path in the complex plane that passes through $t_\pm$ and the use of asymptotic matching to match the solution in the inner region close to $t_\pm$ (which is termed region II), where the waves are generated, to the solution in the outer regions to the left (region I) and to the right (region III) of S_3. We first proceed with the integration near t_+ and consider oscillation-free initial conditions. That is we take the solution in region I to be

$$\hat{p}_I = \frac{2k^2 \hat{q}(0)}{(k^2 + (m - kt)^2)^2}.$$

On the other hand, the solution in region II contains also the generated acoustic waves,

$$\hat{p}_{II} = \frac{2k^2 \hat{q}(0)}{(k^2 + (m - kt)^2)^2} + A\sqrt{K} \mathrm{e}^{(\mathrm{i}/M) \int_0^t K(s)\, \mathrm{d}s} + B\sqrt{K} \mathrm{e}^{-(\mathrm{i}/M) \int_0^t K(s)\, \mathrm{d}s}, \qquad (\mathrm{B}\,1)$$

with amplitudes A, B to be determined.

The path of integration close to t_+ is given by the Stokes lines S_1 and S_2 so that the WKB terms in (B 1) have a constant amplitude at leading order, and the outer

solution following S_1 is

$$\hat{p}_I = \frac{2k^2\hat{q}(0)}{(k^2+(m-kt)^2)^2} \simeq -\frac{\hat{q}(0)}{2k^2(t-t_+)^2}.$$

In order to find the outer solution following S_2, we first calculate the phase integral of the acoustic waves:

$$\int_0^t K(s)\,\mathrm{d}s = \int_0^{m/k} K(s)\,\mathrm{d}s + \int_{m/k}^{t_+} K(s)\,\mathrm{d}s + \int_{t_+}^t K(s)\,\mathrm{d}s \simeq \phi_0 + \mathrm{i}\beta + \frac{2}{3}b^{1/2}\mathrm{e}^{\mathrm{i}\pi/4}(t-t_+)^{3/2}, \tag{B 2}$$

where

$$\phi_0 = \int_0^{m/k} K(s)\,\mathrm{d}s \tag{B 3}$$

is a constant-phase shift, $b=2k^2$ and

$$\beta = \frac{1}{\mathrm{i}}\int_{m/k}^{t_+} K(s)\,\mathrm{d}s = k\int_0^1 \sqrt{1-s^2}\,\mathrm{d}s = k\pi/4.$$

Introducing (B 2) into (B 1), we find that on S_2,

$$\hat{p}_{II} \simeq b^{1/4}\mathrm{e}^{\mathrm{i}\pi/8}(t-t_+)^{1/4}\left(A\mathrm{e}^{\frac{1}{M}(\mathrm{i}\phi_0-\beta+\frac{2}{3}\sqrt{b}\mathrm{e}^{3\mathrm{i}\pi/4}(t-t_+)^{3/2})} + B\mathrm{e}^{\frac{1}{M}(-\mathrm{i}\phi_0+\beta+\frac{2}{3}\sqrt{b}\mathrm{e}^{-\mathrm{i}\pi/4}(t-t_+)^{3/2})}\right) - \frac{\hat{q}(0)}{b(t-t_+)^2}. \tag{B 4}$$

In region III, the WKB approximation to the homogeneous solution (acoustic waves) breaks down at the turning point $t=t_+$. Consequently, we rescale time according to

$$t = t_+ + b^{-1/3}M^{2/3}\tau$$

and $\hat{p}$ by $\hat{p}(\tau)=b^{-2/3}M^{-4/3}f(\tau)$, to obtain the proper balance between the terms in (2.8). Equation (2.8) is then reduced at leading order to

$$\frac{\mathrm{d}^2 f}{\mathrm{d}\tau^2} - \frac{1}{\tau}\frac{\mathrm{d}f}{\mathrm{d}\tau} + \mathrm{i}\tau f = \frac{b^{1/3}\hat{q}(0)}{\mathrm{i}\tau}. \tag{B 5}$$

The solution of (B 5) is given in terms of derivatives of Scorer functions (Abramowitz & Stegun 1965) $\mathrm{Hi}'(r\tau)$ and $\mathrm{Gi}'(r\tau)$, where $r^3=\mathrm{i}$. Using the asymptotic expressions for Hi′ and Gi′ following S_1, that is for $\tau=\mathrm{e}^{-5\mathrm{i}\pi/6}|\tau|$ when $|\tau|\gg 1$, to match the solution of (B 5) to $\hat{p}_I$ on S_1 yields

$$f = \pi b^{1/3}\mathrm{e}^{2\mathrm{i}\pi/3}\hat{q}(0)\mathrm{Hi}'(\mathrm{e}^{-\mathrm{i}\pi/6}\tau). \tag{B 6}$$

The connection formula

$$\mathrm{Hi}'(\mathrm{e}^{-\mathrm{i}\pi/6}\tau) = \mathrm{e}^{-4\mathrm{i}\pi/3}\mathrm{Hi}'(\mathrm{e}^{-5\mathrm{i}\pi/6}\tau) + 2\mathrm{e}^{5\mathrm{i}\pi/6}\mathrm{Ai}'(\mathrm{i}\tau)$$

is subsequently used to find the asymptotic behaviour of (B 6) on S_2 and match with (B 4). Following S_2, $\tau=\mathrm{i}^{-\mathrm{i}\pi/6}|\tau|$, and for $|\tau|\gg 1$ the asymptotic expression of (B 6) becomes

$$f = \pi b^{1/3}\mathrm{e}^{2\mathrm{i}\pi/3}\hat{q}(0)\mathrm{Hi}'(\mathrm{e}^{-\mathrm{i}\pi/3}|\tau|) \simeq \frac{b^{1/3}\mathrm{e}^{-2\mathrm{i}\pi/3}\hat{q}(0)}{|\tau|^2} + \sqrt{\pi}b^{1/3}\mathrm{e}^{5\mathrm{i}\pi/8}\hat{q}(0)\tau^{1/4}\mathrm{e}^{(2/3)\mathrm{e}^{-\mathrm{i}\pi/4}\tau^{3/2}},$$

yielding

$$\hat{p}_{III} \simeq \frac{\mathrm{e}^{-2\mathrm{i}\pi/3}\hat{q}(0)}{b^{1/3}M^{4/3}|\tau|^2} + \sqrt{\pi}b^{-1/3}M^{-4/3}\mathrm{e}^{5\mathrm{i}\pi/8}\hat{q}(0)\tau^{1/4}\mathrm{e}^{(2/3)\mathrm{e}^{-\mathrm{i}\pi/4}\tau^{3/2}}. \tag{B 7}$$

Matching the outer solution (B 4) that is given in terms of the rescaled time τ by

$$\hat{p}_{II} = \frac{\mathrm{e}^{-2\mathrm{i}\pi/3}\hat{q}(0)}{b^{1/3}M^{4/3}|\tau|^2} + b^{1/6}\mathrm{e}^{\mathrm{i}\pi/8}M^{1/6}\tau^{1/4}\left(A\mathrm{e}^{\frac{1}{M}(\mathrm{i}\phi_0-\beta)+\frac{2}{3}\mathrm{e}^{3\mathrm{i}\pi/4}\tau^{3/2}} + B\mathrm{e}^{\frac{1}{M}(-\mathrm{i}\phi_0+\beta)+\frac{2}{3}\mathrm{e}^{-\mathrm{i}\pi/4}\tau^{3/2}}\right)$$

with (B 7) yields

$$[A, B] = \left[0, \frac{\mathrm{i}\hat{q}(0)\sqrt{\pi}\mathrm{e}^{(1/M)(\mathrm{i}\phi_0-\beta)}}{\sqrt{b}M^{3/2}}\right].$$

Following the same procedure, we can find the contribution from t_- and finally obtain the solution given by (4.5).

REFERENCES

Abramowitz, M. & Stegun, I. A 1965 *Handbook of Mathematical Functions*. Dover.

Bakas, N. A. & Farrell, B. F. 2009 Gravity waves in a horizontal shear flow. Part II. Interaction between gravity waves and potential vorticity perturbations. *J. Phys. Oceanogr.* **39**, 497–511.

Bakas, N. A., Ioannou, P. J. & Kefaliakos, G. E. 2001 The emergence of coherent structures in stratified shear flow. *J. Atmos. Sci.* **58**, 2790–2806.

Berry, M. V. 1989 Uniform asymptotic smoothing of Stokes's discontinuities. *Proc. R. Soc. Lond.* A **422**, 7–21.

Blumen, W., Drazin, P. G. & Billings, D. F. 1975 Shear layer instability of an inviscid compressible fluid. Part 2. *J. Fluid Mech.* **71**, 305–316.

Boyd, J. P. 1983 The continuous spectrum of linear Couette flow with the beta effect. *J. Atmos. Sci.* **40**, 2304–2308.

Broadbent, E. G. & Moore, D. W. 1979 Acoustic destabilization of vortices. *Philos. Trans. R. Soc. Lond.* A **290**, 353–371.

Buizza, R. & Palmer, T. N. 1995 The singular vector structure of the atmospheric global circulation. *J. Atmos. Sci.* **52**, 1434–1456.

Butler, K. M. & Farrell, B. F. 1992 Three-dimensional optimal perturbations in viscous shear flow. *Phys. Fluids* A **4**, 1637–1650.

Chagelishvili, G. D., Khujadze, G. R., Lominadze, J. G. & Rogava, A. D. 1997*a* Acoustic waves in unbounded shear flows. *Phys. Fluids* **9**, 1955–1962.

Chagelishvili, G. D., Rogava, A. D. & Segal, I. N. 1994 Hydrodynamic stability of compressible plane Couette flow. *Phys. Rev.* E **50**, R4283–R4285.

Chagelishvili, G. D., Tevzadze, A. G., Bodo, G. & Moiseev, S. S. 1997*b* Linear mechanism of wave emergence from vortices in smooth shear flows. *Phys. Rev. Lett.* **79**, 3178–3181.

Choudhury, S. R. & Lovelace, R. V. E. 1984 On the Kelvin–Helmholtz instabilities of supersonic shear layers. *Astrophys. J.* **283**, 331–342.

Craik, A. D. D. & Criminale, W. O. 1986 Evolution of wave-like disturbances in shear flows: a class of exact solutions of the Navier–Stokes equations. *Proc. R. Soc. Lond.* A **406**, 13–26.

Criminale, W. O. & Cordova, J. Q. 1986 Effects of diffusion in the asymptotics of perturbations in stratified shear flow. *Phys. Fluids* **29**, 2054–2060.

Duck, P. W., Erlebacher, G. & Hussaini, M. Y. 1994 On the linear stability of compressible plane Couette flow. *J. Fluid Mech.* **258**, 131–165.

Ellingsen, T. & Palm, E. 1975 Stability of linear flow. *Phys. Fluids* **18**, 487–488.

Farrell, B. F. 1982 The initial growth of disturbances in a baroclinic flow. *J. Atmos. Sci.* **39**, 1663–1686.

Farrell, B. F. 1984 Modal and non-modal baroclinic waves. *J. Atmos. Sci.* **41**, 668–673.

Farrell, B. F. 1988 Optimal excitation of perturbations in viscous shear flow. *Phys. Fluids* **31**, 2093–2102.

Farrell, B. F. & Ioannou, P. J. 1993*a* Optimal excitation of three-dimensional perturbations in viscous constant shear flow. *Phys. Fluids* A **5**, 1390–1400.

Farrell, B. F. & Ioannou, P. J. 1993*b* Transient development of perturbations in stratified shear flow. *J. Atmos. Sci.* **50**, 2201–2214.

Farrell, B. F. & Ioannou, P. J. 1996 Generalized stability theory. Part I. Autonomous operators. *J. Atmos. Sci.* **53**, 2025–2040.

Farrell, B. F. & Ioannou, P. J. 2000 Transient and asymptotic growth of two-dimensional perturbations in viscous compressible shear flow. *Phys. Fluids* **12**, 3021–3028.

Gustavsson, L. H. 1991 Energy growth of three-dimensional disturbances in plane Poiseuille flow. *J. Fluid Mech.* **224**, 241–260.

Hakim, V. 1998 Asymptotic techniques in nonlinear problems: Some illustrative examples. In *Hydrodynamics and Nonlinear Instabilities* (ed. C. Godreche & P. Manneville), pp. 295–386. Cambridge University Press.

Hanifi, A. & Henningson, D. S. 1998 The compressible inviscid algebraic instability for streamwise independent disturbances. *Phys. Fluids* **10**, 1784–1786.

Hanifi, A., Schmid, P. J. & Henningson, D. S. 1996 Transient growth in compressible boundary layer flow. *Phys. Fluids* **8**, 826–837.

Hardee, P. E. 1979 Configuration and propagation of jets in extragalactic radio sources. *Astrophys. J.* **234**, 47–55.

Hartman, R. J. 1975 Wave propagation in a stratified shear flow. *J. Fluid Mech.* **71**, 89–104.

Ho, C. M. & Huerre, P. 1984 Perturbed free shear layers. *Annu. Rev. Fluid Mech.* **16**, 365–422.

Hu, S. & Zhong, X. 1998 Linear stability of viscous supersonic plane Couette flow. *Phys. Fluids* **10**, 709–729.

Ioannou, P. J. & Kakouris, A. 2001 Stochastic dynamics of Keplerian accretion disks. *Astrophys. J.* **550**, 931–943.

Kelvin, L. 1887 Stability of fluid motion: rectilinear motion of viscous fluid between two parallel plates. *Philos. Mag.* **24**, 188–196.

Kim, J. & Lim, J. 2000 A linear process in wall-bounded turbulent shear flows. *Phys. Fluids* **12**, 1885–1888.

Kreiss, H. O., Lorenz, J. & Naughton, M. J. 1991 Convergence of the solutions of the compressible to the solutions of the incompressible Navier–Stokes equations. *Adv. Appl. Math.* **12**, 187–214.

Landhal, M. T. 1980 A note on an algebraic instability of inviscid parallel shear flows. *J. Fluid Mech.* **98**, 243–251.

Lifschitz, A. & Hameiri, E. 1991 Local stability conditions in fluid dynamics. *Phys. Fluids* A **3**, 2644–2651.

Lindzen, R. S. 1988 Instability of plane parallel shear flow (toward a mechanistic picture of how it works). *Pure Appl. Geophys.* **126**, 103–121.

Mack, L. M. 1965 Computation of the stability of the laminar compressible boundary layer. In *Methods in Computational Physics* (ed. B. Alder, S. Fernbach & M. Rotenberg), pp. 247–299. Academic.

Mack, L. M. 1969 Boundary-layer stability theory. *Tech Rep.* Doc. 900-277. JPL.

Mack, L. M. 1975 Linear stability theory and the problem of supersonic boundary layer transition. *AIAA J.* **13**, 278–289.

Malik, M., Alam, M. & Dey, J. 2006 Nonmodal energy growth and optimal perturbations in compressible plane Couette flow. *Phys. Fluids* **18**, 034103.

Mamatsashvili, G. R. & Chagelishvili, G. D. 2007 Transient growth and coupling of vortex and wave modes in self-gravitating gaseous disks. *Mon. Not. R. Astron. Soc.* **381**, 809–818.

Myers, M. K. 1991 Transport of energy by disturbances in arbitrary steady flows. *J. Fluid Mech.* **226**, 383–400.

Olver, F. W. J. 1974 *Asymptotics and Special Functions*. Academic.

Orr, W. M. F. 1907 The stability or instability of the steady motions of a perfect liquid and of a viscous liquid. *Proc. R. Irish Acad.* A **27**, 69–138.

Papaloizou, J. C. B. & Lin, D. N. C. 1995 Theory of accretion disks. Part I. Angular momentum transport processes. *Annu. Rev. Astron. Astrophys.* **33**, 505–540.

Phillips, O. M. 1966 *The Dynamics of the Upper Ocean*. Cambridge University Press.

Pringle, J. E. 1981 Accretion disks in astrophysics. *Annu. Rev. Astron. Astrophys.* **19**, 137–160.

Reddy, S. C. & Henningson, D. S. 1993 Energy growth in viscous channel flows. *J. Fluid. Mech.* **252**, 209–238.

Reddy, S. C., Schmid, P. J. & Henningson, D. S. 1993 Pseudospectra of the Orr–Sommerfeld operator. *SIAM J. Appl. Math.* **53**, 15–47.

Schmid, P. J. 2007 Nonmodal stability theory. *Annu. Rev. Fluid. Mech.* **39**, 129–162.

Schmid, P. J. & Henningson, D. S. 2001 *Stability and Transition in Shear Flows*. Springer.

Tevzadze, A. G, Chagelishvili, G. D. & Zahn, J. P. 2008 Hydrodynamic stability and mode coupling in Keplerian flows: local strato-rotational analysis. *Astron. Astrophys.* **478**, 9–15.

Trefethen, L. N, Trefethen, A. E., Reddy, S. C. & Driscoll, T. A. 1993 Hydrodynamic stability without eigenvalues. *Science* **261**, 578–584.

Tung, K. K. 1983 Initial value problems for Rossby waves in a shear flow with critical level. *J. Fluid Mech.* **133**, 443–469.

Vanneste, J. & Yavneh, I. 2004 Exponentially small inertia-gravity waves and the breakdown of quasigeostrophic balance. *J. Atmos. Sci.* **61**, 211–223.

Williams, J. E. & Howe, M. S. 1973 On the possibility of turbulent thickening of weak shock waves. *J. Fluid Mech.* **58**, 461–480.

Yamagata, T. 1976 On the propagation of Rossby waves in a weak shear flow. *J. Meteorol. Soc. Jpn* **54**, 126–128.